

AD 739265

IMS

INSTITUTE OF MATERIALS SCIENCE

The research reported in this document has been sponsored by the Air Force Office of Scientific Research under Contract No. F 44620-69-C-0011.
Report dated February 1972.

"Approved for public release; distribution unlimited."

THE UNIVERSITY OF CONNECTICUT
Storrs • Connecticut

Reproduced by
NATIONAL TECHNICAL
INFORMATION SERVICE
Springfield, Va 22151

~~UNCLASSIFIED~~

Security Classification

DOCUMENT CONTROL DATA - R & D

(Security classification of title, body of abstract and indexing annotation must be entered when the overall report is classified)

1. ORIGINATING ACTIVITY (Corporate author)

UNIVERSITY OF CONNECTICUT
DEPARTMENT OF METALLURGY
STORRS, CONNECTICUT 06268

2a. REPORT SECURITY CLASSIFICATION

UNCLASSIFIED

2b. GROUP

3. REPORT TITLE

FRACTURE MECHANICS AND CORROSION FATIGUE

4. DESCRIPTIVE NOTES (Type of report and inclusive dates)

Scientific Interim

5. AUTHOR(S) (First name, middle initial, last name)

ARTHUR J McEVILY ROBERT P WEI

6. REPORT DATE

Feb 1972

7a. TOTAL NO. OF PAGES

51

7b. NO. OF REFS

92

8a. CONTRACT OR GRANT NO

F44620-69-C-0011

8b. PROJECT NO.

9560

c.

61102F

d.

681307

8c. ORIGINATOR'S REPORT NUMBER(S)

8d. OTHER REPORT NO(S) (Any other numbers that may be assigned this report)

AFOSR-TR-72-0408

10. DISTRIBUTION STATEMENT

Approved for public release; distribution unlimited.

11. SUPPLEMENTARY NOTES

TECH, OTHER

12. SPONSORING MILITARY ACTIVITY

AF Office of Scientific Research (NAM)
1400 Wilson Boulevard
Arlington, Virginia

13. ABSTRACT

The development and current state-of-the-art in fracture mechanics in relation to studies of environment-enhanced fatigue-crack growth (corrosion fatigue) and fatigue-crack growth per se are reviewed. Patterns of response of materials to different loading and environmental conditions are considered in terms of the probable mechanisms for environmental embrittlement. The usefulness of the fracture mechanics approach in developing understanding of the mechanisms for fatigue fracture and the engineering utility of this approach are discussed. Areas for additional research are also indicated.

UNCLASSIFIED

Security Classification

14

KEY WORDS

LINK A

LINK B

LINK C

ROLE

WT

ROLE

WT

ROLE

WT

FRACTURE MECHANICS

CORROSION FATIGUE

FATIGUE CRACK GROWTH

ENVIRONMENTAL EFFECTS

UNCLASSIFIED

Security Classification

Approved for public release;
distribution unlimited.

FRACTURE MECHANICS AND CORROSION FATIGUE

A. J. McEvily
Department of Metallurgy
University of Connecticut
Storrs, Connecticut

and

R. P. Wei
Department of Mechanical Engineering and Mechanics
Lehigh University
Bethlehem, Pennsylvania

FRACTURE MECHANICS AND CORROSION FATIGUE

**A. J. McEvily
Department of Metallurgy
University of Connecticut
Storrs, Connecticut**

and

**R. P. Wei
Department of Mechanical Engineering and Mechanics
Lehigh University
Bethlehem, Pennsylvania**

ABSTRACT

The development and current state-of-the-art in fracture mechanics in relation to studies of environment-enhanced fatigue-crack growth (corrosion fatigue) and fatigue-crack growth per se are reviewed. Patterns of response of materials to different loading and environmental conditions are considered in terms of the probable mechanisms for environmental embrittlement. The usefulness of the fracture mechanics approach in developing understanding of the mechanisms for fatigue fracture and the engineering utility of this approach are discussed. Areas for additional research are also indicated.

INTRODUCTION

Fail-safe and safe-life principles provide much of the basis for modern design philosophy, particularly in the aerospace industry. Both of these philosophies recognize that cracks may be present in the structure, or may initiate early in its service life. To maintain structural integrity, it is essential that the inspection interval be chosen carefully so that cracking may be detected promptly, and that the crack tolerance of the material (that is, its fracture toughness) be sufficiently high to resist catastrophic failure. Since crack detection and the residual strengths of structures are both functions of crack size, selection of material and inspection intervals depend on the crack growth and fracture characteristics of the materials. A considerable amount of research has been devoted to the study of these problems during the past fifteen years, and linear elastic fracture mechanics has emerged as the most appropriate framework for these studies.

The purpose of this paper is to review the current state-of-the-art in fracture mechanics, particularly in relation to the study of problems in environment-enhanced fatigue-crack growth, more commonly referred to as "corrosion fatigue."* The usefulness of this approach in developing understanding of the mechanisms for "environmental embrittlement" and its engineering utility will be discussed. Because of the nature of this conference, it appears worthwhile to review briefly the evolution of the fracture mechanics approach and the study of environmental effects on the fatigue behavior of materials.

* Corrosion fatigue shall be defined here as the process of crack growth that requires the conjoint actions of cyclic loading and (chemical) environmental attack.

LIST OF SYMBOLS

K	Stress-intensity factor
ΔK	Stress-intensity factor range
K_I	Stress-intensity factor for Mode I (opening mode) loading
r	Radial coordinate from crack tip (Fig. 2)
σ	Stress
u	Displacement in x-direction
v	Displacement in y-direction
w	Displacement in z-direction
θ	Angular coordinate from the line directly ahead of the crack (Fig. 2)
U	Shear modulus
κ	$3-4\nu$, plane strain; $3-\nu/1+\nu$, plane stress, where ν is Poisson's ratio
E	Young's modulus
G	Strain-energy release rate
G_I	Strain-energy release rate for mode I loading
α	1, plane stress; $\frac{1}{1-\nu^2}$ plane strain
a	Crack length
R	Stress ratio; ratio of minimum to maximum stress in loading cycle
K_c	Fracture toughness
K_{Ic}	Fracture toughness, Mode I (plane strain)
K_{Isc}	Threshold stress intensity under stress-corrosion conditions, Mode I loading
K_{TH}	Threshold stress intensity factor for fatigue loading
COD	Crack-opening displacement
N	Number of cycles
A	Constant of proportionality
σ_y	Yield stress
K_A	Stress-intensity amplitude
K_{max}	Stress-intensity maximum

HISTORICAL BACKGROUND

While much fatigue research has been reported, it is only during the last decade that the deleterious effects of mild environments heretofore considered to be innocuous, such as air, have been fully realized. Thus, the reliability and usefulness of much of the early experimental and design data may be questionable.

The pioneer work on the influence of environment on fatigue was carried out by Haigh [1] and by Gough and Sopwith [2]. These latter workers found that the fatigue lives of most structural metals are significantly reduced by the presence of air (versus vacuum), Figure 1. In later studies [3-14] the reduction of fatigue lives by both liquid and gaseous environments was confirmed on a large number of pure metals and commercial alloys. Fatigue life involves two stages: (1) that of crack initiation followed by limited microcracking along slip planes or grain boundaries (Stage I), and (2) that of the growth of a macroscopic crack (Stage II) [14-16]. Unfortunately, the separate effect of the environment on these two stages cannot be readily ascertained. However, for most high performance engineering structures the presence of cracks having sizes corresponding to the lower limit of detectability of NDT (non-destructive testing) techniques and/or the early initiation of cracks from metallurgical defects are generally assumed. The primary interest, therefore, has been centered on the process of fatigue-crack growth; and specimens containing dominant cracks have been used to study this process.

Fatigue-crack growth per se has been studied extensively both analytically and experimentally over the past two decades. Various continuum models for fatigue-crack growth have been proposed [17-28] and have been discussed in a review paper by Erdogan [29], and by Wei et al [30]. Although some discrepancies

exist between some of these models, there is general agreement on the fact that the mechanical driving force for crack growth is not only a function of the applied stress, but also a function of the crack dimension and component geometry. This dependence has been demonstrated in a systematic experimental study by Weibull [31], and most recently by Feeney et al [32].

The successful application of linear-elastic fracture mechanics analyses to describe fracture behavior of high strength materials under monotonically increasing loads [33] has led to a logical extension of these same concepts to the study of slow crack growth under both sustained (static) and fatigue loads, commonly termed subcritical-crack growth. The use of the crack-tip stress-intensity parameter K (or the strain energy release rate, G), which governs the intensity or magnitude of local stresses, to characterize the mechanical crack-driving force has met with considerable experimental success. The supporting evidence has been documented by Johnson and Paris [34]. A brief review of the basic justification and limitations in using linear-elastic fracture mechanics to describe crack growth and fracture was given by Wei [35] and will be included for the sake of completeness.

Since crack extension and corrosion attack would occur in the highly stressed region at the crack-tip, the stress distribution in the crack-tip region should be considered. The stress fields near crack tips may be divided into three basic types, each associated with a local mode of deformation -- the opening mode, I, and two sliding modes, II and III [36]. The opening mode, mode I, is characterized by direct separation of the crack surfaces symmetrically with respect to the plane occupied by the crack. The edge-sliding mode, II, and the tearing mode, III, are akin to models for edge and screw dislocations respectively. For the present discussion, only the opening mode, I, will be

considered, although the general discussion will be applicable to the other two modes as well.

The stress and displacement fields associated with the opening mode, mode I, in an isotropic elastic body are given by [36-38]:

$$\begin{aligned}
 \sigma_x &= \frac{K_I}{\sqrt{2\pi r}} \cos \frac{\theta}{2} \left[1 - \sin \frac{\theta}{2} \sin \frac{3\theta}{2} \right] \\
 \sigma_y &= \frac{K_I}{\sqrt{2\pi r}} \cos \frac{\theta}{2} \left[1 + \sin \frac{\theta}{2} \sin \frac{3\theta}{2} \right] \\
 \sigma_{xy} &= \frac{K_I}{\sqrt{2\pi r}} \sin \frac{\theta}{2} \cos \frac{\theta}{2} \cos \frac{3\theta}{2} \\
 u &= \frac{K_I}{8\mu} \sqrt{\frac{2r}{\pi}} \left[(2\kappa-1) \cos \frac{\theta}{2} - \cos \frac{3\theta}{2} \right] \\
 v &= \frac{K_I}{8\mu} \sqrt{\frac{2r}{\pi}} \left[(2\kappa+1) \sin \frac{\theta}{2} - \sin \frac{3\theta}{2} \right]
 \end{aligned}
 \tag{1}$$

For plane strain:

$$\kappa = 3 - 4\nu$$

$$\sigma_z = \nu(\sigma_x + \sigma_y)$$

$$w = 0$$

For generalized plane stress:

$$\kappa = \frac{3 - \nu}{1 + \nu}$$

$$\sigma_z = 0$$

$$w = -\frac{\nu}{E} (\sigma_x + \sigma_y) dz$$

r and θ are the radial and angular coordinates measured from the crack tip (Figure 2); μ is the shear modulus; and ν is the Poisson's ratio. Higher order terms in r have been neglected in Equation 1. Hence, the stresses and displacements are to be regarded as good approximations in the region where r is small compared to other planar (x - y plane) dimensions, such as the crack length, and exact in the limit as r approaches zero.

The parameter K_I is the stress intensity factor, for mode I, which depends on the loading and the configuration of the body, including the crack size, and governs the intensity or magnitude of the local stresses. K_I is related to the strain energy release rate G_I through $K_I^2 = \alpha E G_I$, where $\alpha = 1$ for plane-stress; $\alpha = \frac{1}{1 - \nu^2}$ for plane-strain. The analytical determination of the K factors and the crack-tip stress fields is basically a problem in the mathematical theory of elasticity and will not be considered here. K factors for many different loading and body configurations have been catalogued by Paris and Sih [36]. Numerical solutions of K_I for practical test specimens, suitable for routine use, are given in ASTM STP 410 by Brown and Srawley [39].

It should be noted that the linear elasticity solution for a sharp crack (see Equation 1 for example) gives rise to infinite stresses at the crack tip where the radius of curvature is "zero." In reality, of course, the deformed shape of the crack assumes some finite radius of curvature and the stress

level always remains finite. Hence, it is likely that a large deformation theory would predict finite stresses at the crack tip [40]. In addition, the occurrence of local plastic deformation also tends to reduce the stress-concentrating effects of the crack. If the zone of plastic deformation is small in comparison with the crack length and other planar dimensions of the body, then the stress distribution will not be seriously disturbed and the elasticity solutions represent a reasonably accurate approximation of the stress and displacement fields near the crack tip. Since the small zone of plastically deformed material at the crack tip is contained within the surrounding elastic material, it is reasonable to expect that the behavior in this region would be governed by the surrounding elastic material and, thus, be characterized by the crack-tip stress-intensity factor K_I .

Inspection of Equation 1 suggests that identical stress fields are obtained for identical K_I values. Hence, K_I provides a single parameter characterization of the stress and displacement fields near the crack tip, independent of the size of the crack. This is not strictly true, however, since Equation 1 is only approximate for large values of r . The exact analysis of Inglis [41] shows that for cracks of different sizes, for the same K_I , the stresses away from the crack-tip differ considerably; the stresses very close to the crack tip, though, are nearly equal to each other. On the basis of the Inglis solution [41], Liu [42] showed that if the plastically deformed zone is much smaller than some region, within which the elastic stresses are approximately the same for bodies with different sizes of crack loaded to the same level of K_I , the stresses and strains at geometrically similar points, even within the plastic zone, would be the same. Thus, the use of K_I or G_I as a single parameter characterization of the crack driving force may be justified.

It should be emphasized that the use of the crack-tip stress-intensity factor K_I to characterize the crack driving force in practical engineering materials is predicated on the assumption of limited plasticity. The applicability of this approach to actual cases must be established by experimentation. The foregoing discussions are also limited to the case of stationary cracks, in contradistinction to moving cracks that are of concern in subcritical-crack growth. The results of Sih [43] suggest that for the usual rates of crack growth and fatigue loading frequencies encountered in subcritical-crack growth studies, modification of the crack-tip stress-intensity factor K_I to include dynamic effects will not be necessary.

Various types of specimen and loading configurations may be used for studying the effects of environment on subcritical-crack growth. The particular choice of specimen depends principally on the specific application. The more popular specimens are those containing surface flaws (or part-through-cracks) [39, 44, 45], and those containing some form of through-thickness cracks [39, 44]. The surface-flawed specimens are primarily used for service simulation tests, since this type of flaw is most often found in service [45]. Because of the variation of stress-intensity factor K along the crack front [36], the use of this type of specimen for basic studies in subcritical-crack growth will have limited value. In general, those specimens containing a through-thickness crack will be more suitable for these studies. By appropriate specimen design and loading, the stress-intensity factor may be caused to increase, decrease or remain essentially constant with crack prolongation. The particular choice of a given type of specimen and loading will depend on practical considerations of load and space requirements, availability of material, method for containment of test environment, etc. K calibration for the various common types of test specimens and loading configurations are given in ASTM STP 410 [39], along with general guidelines on specimen size

requirements.

Experimental verification of the appropriateness of using K to characterize the mechanical crack driving force was given by Paris [24] and by Feeney et al [32] for fatigue, and by Smith et al [46] for sustained loading. In these experiments, by subjecting specimens containing central-cracks to remote loading and to wedge-force loading (for which K varies in proportion to \sqrt{a} and $1/\sqrt{a}^*$, respectively), the dependence of the rate of crack growth on K is clearly demonstrated [24, 32, 46] (see Figure 3, for example).

* For simplicity, finite-width correction terms are neglected here. In practice, this would correspond to a short crack in a very wide plate.

RESPONSE OF MATERIALS TO FATIGUE AND CORROSION FATIGUE

Characterization of material response and prediction of service performance of structures under fatigue and corrosion fatigue conditions are complicated because of the need to incorporate the multitude of loading variables (such as mean load, cyclic-load amplitude and wave form, and frequency) and their interactions with a range of service environments, and because of the occurrence of delay in crack growth resulting from complex load interactions in variable amplitude loading and the attendant environmental effects. No satisfactory analysis procedure has been developed to date, and methods for material characterization are not well defined. Hence, at present, fatigue-crack growth data, along with stress corrosion cracking information, are used primarily for material selection rather than design.

Much of the early work was directed at assessing the effects of load amplitude, mean load, load range and test frequency on the rate of fatigue-crack growth. This was done to determine material response to the different loading variables and to develop crack growth "laws" for estimating service behavior of structural components [17-28, 31, 46-52]. No formal attempt has been made to incorporate environmental influences into the various crack growth laws [17-28, 46-49]. Experimental work, by and large, was carried out with no environmental control [18, 20, 27, 31, 46-50]. Recent investigations, however, have shown that fatigue-crack growth can be affected strongly by the test environment (even those heretofore regarded as being innocuous, such as air), and that the nature and magnitude of the effect depend on the material-environment interactions involved (i.e., they are dependent on the particular material-environment system) [53-60]. These results indicate that a careful reassessment of the validity and the general applicability of the findings of

the many earlier studies should be made. Such a review of available information up to 1968 was made by Wei [61] and is summarized here along with information that has become available since then.

Experimental information is most complete on the aluminum-water (or water vapor) system. The results indicate that water or water vapor has a strong effect on the rate of fatigue-crack growth in these alloys: 2024-T3, 7075-T6 and T651, 7178-T6, DTD 5070A and DTD 683, and commercially pure aluminum [32, 53-55, 62-65] (see Figure 4 for example).

The effect depends on the partial pressure of water vapor in the atmosphere, and exhibits a transition zone that depends strongly on the test frequency [53, 62, 64], Figure 5. The frequency effect has been attributed to the requirement of a definite amount of surface contamination to achieve full environment effect [66]. These results suggest that a possible mechanism for water-enhanced fatigue-crack growth in the aluminum alloys is the pressure mechanism of hydrogen embrittlement suggested by Broom and Nicholson [67], requiring the synergistic action of fatigue and water-metal surface reaction [55]. Mild frequency dependence for these alloys tested in fully humid environments or in distilled water (reflected by some 50 percent increase in growth rate for nearly a factor of 30 reduction in test frequency) has been attributed to a small contribution from sustained-load crack growth (normally not detectable in a sustained-load test) associated with the increased "time-at-load" at the lower frequencies [61], Figure 4. Environmental sensitivity is reduced at the higher K levels, and appears to result from a reduction in the effectiveness of the pressure mechanism of hydrogen embrittlement associated with "plane-strain" to plane-stress" fracture mode transition [32, 61]. Note that this transition is strictly a reflection of environmental interaction,

since no such transitional behavior has been observed for specimens tested in an inert reference environment (see Figure 6) [61]. At growth rates below 10^{-6} inches per cycle a second type of transition has been observed by McEvily and Illg [19] and by Feeney, et al [32]. The K level at which this transition takes place is associated with the metallurgical structure of the alloy [32] as well as the environment. In the same study [32] it was shown that the effect of a 3.5 percent NaCl solution was approximately the same as that of distilled water for the particular test conditions employed. Although there are significant differences in the rates of fatigue crack growth for the different aluminum alloys (see Figure 7, for example), the response of all of the aluminum alloys to aggressive environments appears to be similar [32, 61].

The rate of fatigue-crack growth is affected by the "stress ratio" R ($R = K_{\min} / K_{\max}$ in a given cycle of loading) in both the inert and the aggressive environments, Figure 8. This effect is reasonably accounted for by the Forman equation, although the general validity and range of applicability of this relationship is in question [51, 63]. Fatigue-crack growth can depend strongly on temperature in both the inert and aggressive environments [55], the dependence being a function of K or ΔK . Experimental results obtained by Wei [55] for a 7075-T651 aluminum alloy suggest that fatigue-crack growth in the aluminum alloys is thermally activated with apparent activation energies that depend strongly on K. A careful examination of the effect of K on the apparent activation energies could provide a means for estimating the very low rates of crack growth that cannot be obtained readily in normal testing.

Comparable data for fatigue-crack growth in the titanium alloys and high-strength steels in water or water vapor, and in salt solution are more limited. Available data on these systems indicate that the behavior is quite different

from that of the aluminum-water system [56, 58-61, 68-75]. The dependence on test frequency can be very strong and appears to be related to the environment sensitivity of the alloy [59, 60, 68-75]. The environment sensitivity, in turn, depends on the alloy composition and microstructure (or heat treatment). No appreciable synergistic effects of fatigue and corrosion were apparent at K levels above some apparent threshold value. Below this apparent threshold K, recent experimental results suggest that some synergistic effect may be present and that the effect may be influenced by the wave form of the applied load [74-75].* Specimen thickness appears to have less influence on environmental sensitivity than in the case of the aluminum-water system [61]. (However, a reduction in environmental sensitivity at high K levels may well be expected, depending on the mechanism of embrittlement).

Recent studies have led to the suggestion of a simple, quantitative method for estimating the effect of aggressive environments on fatigue-crack growth in some ultrahigh-strength steels [72]. This suggestion was based on an accumulation of experimental evidence and fractographic observations that indicated that the mechanism for environmental enhancement of fatigue-crack growth is the same as that for crack growth under sustained loads. In this method, the rate of fatigue-crack growth in an aggressive environment is considered to be the sum of the rate of fatigue-crack growth in an inert reference environment and an environmental component to be computed from the load profile and sustained-load crack growth data obtained in an identical

* No effect of wave form was noted in the case of aluminum alloys tested in humid environment [76, 77].

aggressive environment.* Experimental results have shown that this simple superposition method correctly predicts the effects of test frequency and mean load or stress ratio, at K levels above some apparent threshold value, for ultrahigh-strength steels tested in gaseous hydrogen, distilled water, and water vapor environments, and for a Ti-8Al-1V-1Mo alloy tested in distilled water and salt solution [61, 72-74]. These results suggest that the apparent influences of metallurgical structure reported by Miller [70] are principally reflections of the environment sensitivities of the individual steels.

The ability to predict the rates of fatigue-crack growth in an aggressive environment for different loading conditions directly from two sets of laboratory data (that for sustained-load crack growth in the aggressive environment and that for fatigue-crack growth in an inert reference environment) is of obvious engineering significance. It would not only reduce, drastically, the amount of testing needed for material characterization, but also provide a useful basis for the development of meaningful procedures for estimating the serviceable lives of engineering structures. Further extensions of this method should be carefully explored. Since the below-threshold effects reported by Barsom [78], like those for the aluminum alloys, cannot be accounted for by this method, further refinements and modifications of this analysis procedure will be needed.

Although hydrogen embrittlement or embrittlement by chloride ions has been inferred from experimental results on water- and salt-water-enhanced crack

* A similar model had been suggested by McEvily and Bond [57] for corrosion fatigue of α -brass in a tarnishing solution. The sustained load component was identified with the rate of film formation which was assumed to be stress independent. In the model considered by Wei and Landes [72] no specific mechanism was postulated and the crack velocity was taken to be dependent on K.

growth in these alloys, the precise mechanism(s) have not been established. For example, studies of water-enhanced crack-growth under sustained loads in medium carbon, low-alloy ultrahigh-strength steels were carried out by Johnson and Willner [79], Hancock and Johnson [80], Hanna et al. [81], and Van der Sluys [82]. These workers suggested that the plausible mechanism for water-enhanced crack growth in these steels is hydrogen embrittlement [83, 84]. Wei, Talda and Li [59] suggested that oxidation per se should not be ruled out on the basis of their fatigue-crack growth studies (which included two tests in a bromine vapor environment). Fractographic observations reported by Spitzig, Talda and Wei [60] showed that the paths of fracture for specimens tested in "dry" hydrogen and in the moist environments are different and provide a further basis for questioning the validity of the suggested hydrogen embrittlement mechanism. Further mechanistic studies are needed to develop information useful to new alloy development and for clarification of the response of materials to corrosion fatigue.

Metallurgically, Wei et al. [59] and Miller and Wei [74] showed that the rates of fatigue-crack growth in an inert environment are nearly the same for several ultrahigh-strength steels, independent of the chemical composition and heat treatment (or microstructure). However, the rates of fatigue-crack growth in a moist environment or in distilled water are different, and appear to be related to the fracture toughness and environment sensitivity of the alloy.

The results of these various studies may be summarized in terms of behavior patterns and thermal variables.

1. Behavior Patterns

The fatigue-crack growth response of materials in an inert environment is illustrated in Figure 9. The rate of crack growth depends strongly on K at

K levels approaching K_C or K_{IC} at the high end and at levels approaching an apparent threshold at the lower end, with an intermediate region that depends on some power of K or ΔK of the order of 2 to 10. The upper end corresponds to the onset of unstable fracturing, while the lower end corresponds to some apparent limiting K level for crack growth, which appears to be related to the metallurgical structure [19, 32].

The environment-enhanced fatigue-crack growth response of high-strength metals may be broadly characterized in terms of three general patterns of behavior as illustrated schematically in Figure 10. The first type of behavior (hereafter referred to as Type A), represents those material-environment systems where the environmental effect results from the synergistic actions of fatigue and corrosion. This behavior pattern is typified by that of the aluminum-water system [61]. The environmental effect is evidenced by a reduction in the apparent threshold for crack growth and increases in the rate of crack growth at given K levels. As K approaches K_C or K_{IC} the environmental influences are diminished as a result of either the rate limiting nature of transport processes or other mechanical-chemical interactions. The second type of behavior (Type B) typified by the hydrogen-steel system [60, 72] represents those systems where there is a substantial environment-enhanced sustained-load crack growth component [61, 72]. The environmental effects are quite strong above some apparent threshold for "stress-corrosion cracking" (K_{ISCC}) and are negligible below this level. A broad range of material-environment systems exhibit behavior that falls between these two extremes (Type C), with Type A behavior at K levels below the apparent threshold K level and Type B behavior above this threshold. The response of materials to the various mechanical loading variables will depend largely on the type of behavior patterns observed, and will be discussed below.

2. Test Frequency

In considering the effect of test frequency, it is important to distinguish between that which is "intrinsic" to the materials (i.e., due to rate sensitivity of the material) and that which is caused by interactions with the test environment. Experimental evidence obtained to date suggest that there is essentially no intrinsic frequency effect for most high-strength structural metals over a range of test frequencies from 1/60 to 150 Hz., and that the observed frequency dependence is strictly related to environment interactions [32, 61, 64, 65, 69, 72]. For the aluminum-water systems, the frequency effect is strongly affected by the partial pressure of water vapor in partially saturated gaseous environments and is quite small in the fully saturated environment and in water [32, 61, 63]. For material-environment systems that exhibit Type B behavior, Figure 10(b), the magnitude of the frequency-effect will depend on the environment sensitivity of the alloy. For a 10Ni steel and a Ti-8Al-1V-1Mo alloy tested in salt solution, Barsom [75] and Bucci [69] reported that there appears to be some test frequency for which the environmental effect on fatigue-crack growth below some threshold K is a maximum. These frequency effects should be systematically examined.

3. Stress Ratio

The rate of fatigue-crack growth is affected by the stress ratio R in both the inert and the aggressive environments. For material-environment systems that exhibit Type A behavior, the influence of R on crack growth in an aggressive environment is comparable with that for the inert environment, although the "plane-strain" to "plane-stress" transition point is expected to be altered. In the case of material-environment systems that show Types B and C behavior, the effect of R can be large, since it affects the period for which K is above some threshold level during a given load cycle.

4. Wave Form

The influence of cyclic-load wave form on fatigue-crack growth has not been explored extensively. For Type B and C systems, an effect of wave form would be expected on the basis of the simple superposition model suggested by Wei and Landes [72]. It is less clear in the case of Type A systems. Barsom [78] reported that wave form can have a significant effect on the rate of fatigue-crack growth in a 10Ni steel in a K range where Type A behavior was observed. However, experiments by Bradshaw et al. [76] and by Hudak and Wei [77] on aluminum alloy, using some of the same wave forms, indicate no effect of wave form. Clearly the effect of wave form may be peculiar to specific material-environment systems. Since various cyclic-load wave forms are currently employed in fatigue testing, this aspect of the problem should be explored more closely.

5. Specimen Thickness

The effect of specimen thickness (or more appropriately the relative thickness - the ratio between specimen thickness and some measure of the crack-tip plastic zone size), on fatigue-crack growth and fatigue-life is complicated. It influences fatigue behavior through its effect on the fracture toughness, K_{IC} , as well as through its influence on the apparent environment sensitivity of the material associated with a "plane-strain" to "plane-stress" fracture mode transition. These concomitant effects are difficult to assess and should be considered.

6. Temperature

Experimental evidence has shown that the rate of fatigue-crack growth can be affected strongly by temperature [55, 85]. The temperature dependence may be related to the deformation properties of the material or may be related to the

environment-metal interactions that produce embrittlement. Since structures are often expected to operate over a wide range of temperatures, inclusion of temperature as a test variable should be considered in addition to its value as an independent variable for mechanistic studies.

MECHANISMS AND MODELING

The mechanisms of the fatigue process can be conveniently considered in terms of the individual component stages of crack initiation and crack growth. Of these stages, the simplest with which to deal in an analytical manner is that of crack growth in the absence of environmental effects. For this case, semi-empirical expressions can be derived based upon a process of crack growth which is purely mechanical. The influence of the environment can then be considered in terms of its effect on this basic process. Let us begin by considering the mechanical aspects of the growth process.

Overall characteristics of fatigue crack growth have been indicated in Figure 9. Crack growth rates range from zero for values of the stress intensity factor less than K_{TH} , up to inches per cycle for stress intensity factors approaching K_C . Over this range two distinct mechanical modes of crack advance may be operative, each in a particular region. For growth rates below about 10^{-4} inches per cycle the mechanism may be as indicated in Figure 11. In this mechanism crack growth per cycle occurs as the result of a repetitive process of crack tip blunting followed by resharpener. It is this process which creates the characteristic fatigue markings on the fracture surface, although these markings are sometimes difficult to observe, as with high strength aluminum alloys tested in vacuum [86]. Above 10^{-4} inches per cycle in the

case of high strength alloys the mechanism may gradually shift to one of ductile tearing [87] giving rise to the presence of dimples on the fracture surface. This mode of separation will result in complete failure at the K_c level. However, with low strength materials such as copper or pure aluminum this tearing mode may not be operative until complete failure occurs.

A recent paper has dealt with the blunting and resharpening process in a quantitative manner [88]. In the approach employed it is assumed that the advance per cycle is proportional to the crack-opening displacement (COD) which in turns depends upon K^2 . A modification is introduced to account for the existence of the threshold level, K_{TH} , which leads to the following expression for the rate of crack growth per cycle for $R = 0$ loading:

$$\frac{\Delta a}{\Delta N} = \frac{4A}{\pi \sigma_y E} (K_{max}^2 - K_{TH}^2) \quad \text{Eq. (2)}$$

Predicted rates based upon this equation were found to be in reasonably good agreement with experiment, e.g., Figure 12. In the context of the present conference it is of particular interest to note that for tests in vacuum, the constant A can be expressed as

$$A = 2\sigma_y/E, \quad \text{Eq. (3)}$$

that is A is twice the yield strain. Upon substitution of this result into Eq. 2 one obtains:

$$\frac{\Delta a}{\Delta N} = \frac{8}{\pi} \left[\left(\frac{K_{max}}{E} \right)^2 - \left(\frac{K_{th}}{E} \right)^2 \right] \quad \text{Eq. (4)}$$

where K/E is the strain intensity factor. On this basis both Young's modulus and K_{TH} appear to be important material parameters affecting crack growth by

mechanical processes. The yield strength, however, is still a factor, for in this approach it is assumed that the net section stresses are well below the yield level.

The influence of an aggressive environment is seen through its effect upon the constants A and K_{TH} of Eq. 2. A corrosive environment causes A to increase and K_{TH} to decrease. Nothing is said however about the details of the effect of the environment upon the mechanism of growth, although a number of factors may be of importance. For example, plastic deformation at a notch root in an aggressive environment can result in greatly enhanced and localized dissolution [89]. Absorption of hydrogen at local cathodes may lead to hydrogen embrittlement and consequent acceleration of crack growth. Which, if either, of these processes is controlling in a given situation is certainly an area for further research, and since we are not yet in a position to treat environmental effects in a detailed sense, other predictive approaches are of interest. To date these approaches have been based upon a linear superposition of corrosion or stress-corrosion effects upon the mechanical fatigue process. The following expression due to Wei and Landes [72] is an example of this type of simple approach:

$$\left(\frac{\Delta a}{\Delta N}\right)_c = \left(\frac{\Delta a}{\Delta N}\right)_r + \int \frac{da}{dt} \cdot k(t) dt \quad \text{Eq. (5)}$$

where $\left(\frac{\Delta a}{\Delta N}\right)_c$ is the rate of fatigue-crack growth in an aggressive environment, $\left(\frac{\Delta a}{\Delta N}\right)_r$ is the rate of fatigue-crack growth in an inert environment, and the integral term is the environmental component computed from sustained-load crack growth data obtained in the same aggressive environment. Such an approach is applicable when Type B behavior, Fig. 10, is observed, since it predicts that

below K_{Iacc} level there is no environmental effect. Figure 13 compares results of experiments with predictions made on this basis.

A related approach has been used to account for frequency effects on the corrosion fatigue behavior of α -brass tested in a tarnishing solution [57]. In this case it is postulated that a tarnish film forms at the tip of the crack in each cycle, and the thickness of this film per cycle is estimated on the basis of macroscopic kinetics. Superposition of the corrosion reaction upon the mechanical process of crack advance leads to

$$\frac{\Delta a}{\Delta N} = \frac{8}{\pi} \left[\left(\frac{K_{max}}{E} \right)^2 - \left(\frac{K_{TH}}{E} \right)^2 \right] + b(f) \quad \text{Eq. (6)}$$

where $b(f)$ represents the amount of tarnish formed per cycle, a function of the frequency, f . Fair agreement between calculated and predicted lifetimes was obtained using this approach.

Both of the above models are grossly oversimplified, but are of interest as first order approximations. An improvement on such models will require the incorporation of reaction kinetics which are able to account for effects associated with the exposure of new and possibly highly reactive fracture surface to the environment during each loading cycle.

APPLICATIONS

For the case of constant amplitude loading, once information is available on the rate of crack growth as a function of the stress intensity factor, it is, in principal, a straightforward matter to determine residual fatigue lifetime by integration of the rate expression between the limits of the initial and final flaw sizes. However, in practice the procedure may not be so simple. In many cases of interest, random loading, involving history effects, may be involved. In addition if the crack is growing in a part of

complex geometry, the stress intensity factor may not be known. With this caveat, a simple case can provide an illustration of the potential of the method. In the particular case of a through-slit in a sheet specimen subjected to pulsating tension loading perpendicular to the slit, integration of Eq. 2 leads to

$$N = \frac{\sigma_y E}{4A\sigma^2} \ln \left[\frac{K_F^2 - K_{TH}^2}{K_I^2 - K_{TH}^2} \right] \quad \text{Eq. (7)}$$

where in this case $K = \sigma_{\max} \sqrt{\pi a}$, and K_F and K_I are the final and initial stress intensity factors, corresponding to a_f and a_i , the final and initial crack lengths. Figure 14 shows crack growth curves computed on this basis. It is noted that insofar as the total life is concerned the precise value of a_f is relatively unimportant provided that $a_f \gg a_i$. In this example the growth curves have been terminated where the rate of crack growth attains a value of 10^{-4} inches per cycle. Such calculations are useful in comparing materials and perhaps in setting inspection schedules. However, we are not yet able to make reliable calculations of crack growth where variable amplitude loading is involved.

Thus far the discussion has primarily been concerned with crack growth under $R = 0$ loading conditions. One reason for this emphasis is that most crack growth data are obtained under conditions which approximate this type of loading. Other types of constant amplitude loading are also of interest, but in considering them it is convenient to use the $R = 0$ loading as a base, and, therefore, the constants A and K_{TH} of Eq. 2 are determined for this condition. For R ratios other than zero, Figure 15 [90] indicates how predictions of crack growth rates, and hence lifetimes, can be made once

growth rates for $R = 0$ are known. This figure is a growth rate equivalent of the Goodman diagram. (It will be recalled that in the Goodman diagram the stress amplitude for a given lifetime is plotted as a function of the mean stress). In Figure 15, a break is noted in the solid lines about the $R = 0$ line. For loading to the left of this line, the specimen is in compression during a portion of the cycle. If this portion is ineffective in advancing the crack then we would expect that the K_{AMP} corresponding to $R = -1$ loading would be twice that for $R = 0$ loading. However, at higher amplitudes in this range compression may be effective in resharpening the crack and thereby increasing the rate of crack growth. At this time a conservative estimate of growth rates in the compression portion of the diagram can be obtained by working with the dashed lines on Figure 15.

The following expressions based upon this idealized diagram can be used to estimate the effect of R ratio on the rate of crack growth. It is assumed that knowledge of the rate of growth under $R = 0$ conditions is available, i.e., the constants A and K_{TH} of Eq. 2 for the environment under consideration are known. The stress-intensity amplitude, K_A , at any R value for a given rate of crack growth can be related to the stress-intensity amplitude for $R = 0$, K_{A_0} , at this same rate of growth by the following relation:

$$K_A = \frac{K_{A_0} K_C (1-R)}{K_C (1-R) + 2R K_{A_0}} \quad \text{Eq. (8)}$$

where K_C is the fracture toughness.

Since

$$K_{A_0} = \frac{1}{2} \left(\frac{\pi \sigma_y E}{4A} \frac{\Delta a}{\Delta N} + K_{TH}^2 \right)^{1/2},$$

the following expression for the rate of crack growth at any R value can be obtained:

$$\frac{\Delta a}{\Delta N} = \frac{4A}{\pi \sigma_y E} \left\{ \left[\frac{2K_A}{1 - \left(\frac{2R}{1-R} \right) \frac{K_A}{K_C}} \right]^2 - K_{TH}^2 \right\} \quad \text{Eq. (9)}$$

The variation of the threshold value of the stress-intensity amplitude, K_{ATH} , as a function of R is given by:

$$K_{ATH} = \frac{K_{ATH_0}}{1 + \left(\frac{2R}{1-R} \right) \frac{K_{ATH_0}}{K_C}}, \quad \text{Eq. (10)}$$

where K_{ATH_0} is the stress-intensity amplitude at the threshold level for $R = 0$ loading, i.e., it is equal to one-half K_{TH} .

The objective of such an approach is to minimize the amount of testing required. Knowledge of but two material constants, A and K_{TH} , (which are tabulated for a number materials in Ref. 88) enables one to make predictions of growth rate for various R values. Such procedures should be useful to design engineers.

It may also be of interest to consider the application of knowledge of fatigue crack growth to the prediction of the high-cycle life of unnotched specimens. There is evidence that in some materials cracks form at inclusions or slip bands at a very small fraction of the total fatigue life. In some cases these cracks do not propagate past the first grain boundary encountered [91]. In such a case the lowest stress level at which propagation past the boundary can occur may correspond to the endurance limit or run-out life of the

material. In the growth stage from some initial size a_0 , the rate of growth and the associated stress intensity factor will depend upon the applied stress. As the crack lengthens to the grain size (or some other barrier length) it will experience some difficulty in being able to propagate into the next grain. That is, the stress intensity factor may have to exceed some characteristic level which we take to be equivalent to K_{TH} . If the stress intensity at the barrier length, a_b , is less than K_{TH} a condition for the non-propagation of a crack exists, as is indicated in the schematic crack growth curves of Figure 16.

In order to make calculations of the stress intensity in this range, information is needed concerning the orientation and shape of the crack at size a_b . In the absence of such detailed information a flaw "equivalent" to a through crack in a sheet specimen will be used. In this treatment the value of a_b is equal to $K_{TH}^2 / \pi \sigma_{TH}^2$, where σ_{TH} is the stress at the run-out level of the S-N curve. The following expressions [92] can be used to compute the number of cycles spent in this first stage of growth:

$$\frac{\Delta a}{\Delta N} = \frac{4A}{\sigma_y E} \left(K^2 - K_{TH}^2 \frac{K_{TH}}{K_{a_b}} \frac{a}{a_b} \right) \quad \text{Eq. (11)}$$

which for $K = \sigma \sqrt{\pi a}$ leads to

$$N_I = \frac{\sigma_y E}{4A} \left(\frac{1}{\sigma^2 - K_{TH}^2 \frac{K_{TH}}{\sigma \sqrt{\pi a_b}} \frac{1}{a_b}} \right) \ln \frac{a_b}{a_0} \quad \text{Eq. (12)}$$

In this analysis it is assumed that threshold effects at the start of this stage can be neglected. The last term in Eq. 11 is introduced to allow for growth of the type shown for curve C, Figure 16.

The number of cycles spent in the next stage, N_{II} , is given by

$$N_{II} = \frac{\sigma_y E}{4A\sigma^2} \ln \left(\frac{\sigma^2 \pi a_f^2 - K_{TH}^2}{\sigma^2 \pi a_b^2 - K_{TH}^2} \right) \quad \text{Eq. (13)}$$

The total life is then given by

$$N = N_I + N_{II} \quad \text{Eq. (14)}$$

Results of calculations carried out on this basis for an aluminum alloy are shown in Fig. 17. An "equivalent" barrier flaw size, a_b , of 0.01 inches was used. A smaller value would shift the computed curves to a higher level to even closer agreement with experiment. The curve for $a_0 = a_b$ clearly underestimates the total life in the finite life range as expected, for in this case there would be no stage I growth. As the value of a_0 decreases the contribution of N_I to the total life increases and the calculated curves approach the experimental curve. The effect of a more aggressive environment would be to reduce the stress required for propagation at a_b because of the corresponding reduction in K_{TH} . Such a reduction would be in accord with the reduction in fatigue life shown in Figure 1.

This approach is as yet at an early stage. A potential use is to minimize the amount of testing required in the determination of the minimum life edge of the scatter band at some predetermined probability of failure level. Such a development would, of course, be of interest to the designer concerned with fatigue in aggressive environments.

SUMMARY

In this paper we have attempted to bring out the role of fracture mechanics in the study of the corrosion fatigue process. It is not expected that this approach will supplant other approaches in the dealing with corrosion fatigue problems, rather it is considered to be another useful tool at the disposal of the engineer concerned with this type of problem. The approach is still in its early stages. However, its rational nature and the fact that it lends itself more readily to mathematical treatment for use in making predictions than to some other approaches, say, based on total life, make it appear that its utilization will increase in time. We are very rapidly sketching out the borders of the overall picture of fatigue as influenced by corrosion, and in this process some answers have already been provided. However, especially for those concerned with the details of the processes involved, the answers are still some time off. In the area of providing useful engineering approaches we are much closer to being effective. When one looks back at the remarkable advances made over the past twenty years in our understanding of fatigue, one cannot be but optimistic about the future application of this knowledge.

ACKNOWLEDGMENT

We would like to acknowledge the support given to this study by the Air Force Office of Scientific Research (A.J.M.), and the Advanced Research Projects Agency, Department of Defense, (under Contract Nonr 610 (09)), and the National Aeronautics and Space Administration (R.P.W.).

REFERENCES

1. B. P. Haigh, J. Inst. Metals, 18, 55 (1917).
2. H. J. Gough and D. G. Sopwith, J. Inst. Metals, 49, 93 (1932).
3. N. J. Wadsworth and H. Hutchings, Phil. Mag., 3, 1154 (1959).
4. N. J. Wadsworth, in Internal Stresses and Fatigue in Metals, Elsevier Publishing Co., 382 (1959).
5. T. Broom and A. Nicholson, J. Inst. Metals, 89, 183 (1961).
6. J. A. Bennett, in Fatigue of Aircraft Structures - Proceedings of the Paris Symposium, W. Barrois and E. L. Ripley, editors (1961).
7. J. L. Ham and G. S. Reichenbach, "Fatigue Testing of Aluminum in Vacuum and the Effect of Pressure on Life and Surface Appearance," paper presented at Fourth Pacific National Meeting of ASTM (1962).
8. G. A. Jenkins and W. T. Roberts, "The Atmospheric Corrosion-Fatigue and Stress Corrosion Properties of Commercial High Strength Aluminum Alloy Extrusion," S and T Memo 14162, Min. of Aviation (Great Britain).
9. I. R. Kramer and G. E. Podlaseck, "Behavior of Metals in Vacuum," Martin Co. Res. Memo 102, (October 1961).
10. J. A. Bennett, J. Res., Nat. Bur. Std., 68C, 91 (1964).
11. J. A. Bennett, in Fatigue - An Interdisciplinary Approach, Syracuse University Press, 209 (1964).
12. M. R. Achter, G. L. Danek, Jr., and H. H. Smith, Trans. Met. Soc. AIME, 227, 1246 (1963).
13. J. A. Bennett, Acta Met., 11, 799 (1963).
14. C. Laird and G. C. Smith, Phil. Mag., 8, 1945 (1963).
15. P. J. E. Forsyth, in Proceedings of the Crack Propagation Symposium, Vol. I, College of Aeronautics, Cranfield, England, 76 (September 1961).
16. C. Laird, ASTM STP 415, 131 (1967).
17. A. K. Head, Phil. Mag. 44, 925 (1953).
18. N. E. Frost and D. S. Dugdale, J. Mech. Phys. Solids, 6, 92 (1958).
19. A. J. McEvily and W. Illg, NACA TN 4394 (1958).
20. H. W. Liu, J. Basic Eng'g., Trans. ASME, 83, 23 (1961).

21. P. C. Paris and F. Erdogan, J. Basic Eng'g., Trans. ASME, 85, 528 (1963).
22. H. F. Hardrath and A. J. McEvily, in Proceedings of the Crack Propagation Symposium, College of Aeronautics, Cranfield, England (September 1961).
23. F. A. McClintock (discussion), in ASTM STP 415, 170 (1968).
24. P. C. Paris, in Fatigue - An Interdisciplinary Approach, Syracuse University Press, 107 (1964).
25. J. M. Krafft, Trans. ASM, 58, 691 (1965).
26. J. M. Krafft, (discussion), ASTM STP 415, 483 (1967).
27. A. J. McEvily and T. L. Johnston, International Conference on Fracture, Sendai, Japan (September 1965).
28. J. Weertman, *ibid.*
29. F. Erdogan, in Fracture - An Advanced Treatise, Vol. II, H. Liebowitz, editor, Academic Press (1970).
30. R. P. Wei, P. M. Talda and Che-Yu Li, ASTM STP 415, 460 (1967).
31. W. Weibull, Acta Met., 11, 745 (1963).
32. J. A. Feeney, J. C. McMillan and R. P. Wei, Met. Trans., 1, 1741 (1970).
33. Anon., ASTM STP 381 (1965).
34. H. H. Johnson and P. C. Paris, J. Eng'g. Frac. Mech., 1, 3 (1968).
35. R. P. Wei, in Proceedings of Conference - Fundamental Aspects of Stress Corrosion Cracking, Ohio State University, 104 (1969).
36. P. C. Paris and G. C. Sih, in ASTM STP 381, 30 (1965).
37. G. R. Irwin, J. Appl. Mech., Trans. ASME, 79, 361, (1957).
38. G. R. Irwin, in Structural Mechanics, Pergamon Press, 557 (1960).
39. W. F. Brown, Jr. and J. E. Srawley, ASTM STP 410 (1966).
40. G. C. Sih and H. Liebowitz, in Fracture - An Advanced Treatise, Vol. II, H. Liebowitz, editor, Academic Press (1970).
41. E. E. Inglis, Trans., Institution of Naval Architects (London), 60, 219 (1913).
42. H. W. Liu, (discussion), in ASTM STP 381, 23 (1965).
43. G. C. Sih, Int'l. J. Fract. Mech., 4 (1968).

44. B. F. Brown and C. D. Beachem, Corrosion Science, 5, 745 (1965).
45. C. F. Tiffany and J. N. Masters, in ASTM STP 381, 249 (1965).
46. H. W. Liu, Trans. ASME, Ser. D, 85, 116 (1963).
47. H. W. Liu, Appl. Mat'l. Res., 3, 229 (1964).
48. W. Illg and A. J. McEvily, NASA TN D-52 (1959).
49. D. Broek and J. Schijve, NLR TN M. 2111 (1963).
50. J. Schijve, in ASTM STP 415, 514 (1967).
51. R. G. Forman, V. E. Kearny and R. M. Engle, Trans. ASME, Ser. D, 88, 459 (1967).
52. R. Roberts and F. Erdogan, Trans. ASME, Ser. D, 89, 885, (1967).
53. F. J. Bradshaw and C. Wheeler, Appl. Mat'l. Res., 5, 112 (1966).
54. A. Hartman, Int'l. J. Fract. Mech., 4, 167 (1965).
55. R. P. Wei, Int'l. J. Fract. Mech., 4, 159 (1968).
56. E. P. Dahlberg, Trans. ASM, 58, 46 (1965).
57. A. J. McEvily and A. P. Bond, in Environment Sensitive Mechanical Behavior, AIME, 35, (1966).
58. Che-Yu Li, P. M. Talda and R. P. Wei, Int'l. J. Fract. Mech., 3, 29 (1967).
59. R. P. Wei, P. M. Talda and Che-Yu Li, in ASTM STP 415, 460 (1967)
60. W. A. Spitzig, P. M. Talda and R. P. Wei, J. Eng'g. Fract. Mech., 1, 155 (1968).
61. R. P. Wei, J. Eng'g. Fract. Mech., 1, 633 (1970).
62. A. Hartman, F. J. Jacobs, A. Nederveen and R. DeRijk, NRL TN M. 2182 (May 1967).
63. A. Hartman and J. Schijve, NLR MP 68001U (1968).
64. F. J. Bradshaw and C. Wheeler, RAE TR-68041 (February 1968).
65. R. P. Wei and J. D. Landes, Int'l. J. Fract. Mech., 5, 69 (1969).
66. F. J. Bradshaw, Scripta Met., 1, 41 (1967), and RAE Tech. Memo. MAT 26 (March 1968).
67. T. Broom and A. J. Nicholson, J. Inst. Metals, 89, 183 (1960).

68. D. A. Meyn, Rept. NRL Progress, 14 (February 1968).
69. R. Bucci, "Environment Enhanced Fatigue and Stress Corrosion Cracking of a Titanium Alloy Plus a Simple Model for Assessment of Environmental Influence of Fatigue Behavior," Ph.D. dissertation, Lehigh University (1970).
70. G. A. Miller, Trans. ASM, 61 (1968).
71. W. A. Spitzig and R. P. Wei, J. Eng'g. Fract. Mech., 1, 719 (1970).
72. R. P. Wei and J. D. Landes, Mat'l. Res. and Std., ASTM, 9, 25 (July 1969).
73. J. D. Landes, "Kinetics of Subcritical-Crack Growth and Deformation in a High-Strength Steel," Ph.D. dissertation, Lehigh University (1970).
74. G. A. Miller and R. P. Wei, "Some Experiments on the Effects of Testing Variables and Environment on Fatigue-Crack Growth in 4340 Steel," presented at ASTM Committee E-24 meeting in Philadelphia, (October 7, 1970).
75. J. M. Barsom, "Investigation of Subcritical-Crack Propagation," Ph.D. dissertation, University of Pittsburgh (1969).
76. F. J. Bradshaw, N. J. F. Nunn and C. Wheeler, RAE Tech. Memo. MAT 93 (July 1970).
77. S. Hudak and R. P. Wei, unpublished results (1970).
78. J. M. Barsom, "Effect of Cyclic Stress Form on the Corrosion Fatigue Crack Propagation Below K_{Isc} ," this conference.
79. H. H. Johnson and A. M. Willner, Appl. Mat'l. Res., 4, 34 (1965).
80. G. G. Hancock and H. H. Johnson, Trans. Met. Soc. AIME (April 1966).
81. G. L. Hanna, A. R. Troiano and E. A. Steigerwald, Trans. ASM, 57, 658.
82. A. W. Van der Sluys, Trans. ASME, Ser. D, 89, 28 (1967).
83. H. H. Johnson, Proceedings of Conference - Fundamental Aspects of Stress Corrosion Cracking, Ohio State University, 439 (1969).
84. A. S. Tetelman and W. D. Robertson, Acta. Met., 11, 415 (1963).
85. J. T. Ryder and J. P. Gallagher, Trans. ASME, 92, Series D, 121 (1970).
86. D. A. Meyn, cited by M. R. Achter in ASTM STP 415, 181 (1967).
87. R. W. Hertzberg, Fatigue Crack Propagation, ASTM STP 415, 205 (1967).
88. R. J. Donahue, H. McI. Clark, P. Atarmo, R. Kumble, and A. J. McEvily, to be published in the Int. J. of Fracture Mechanics.

89. R. G. Weber and A. J. McEvily, Fracture 1969, Proc. 2nd Int. Conf. on Fracture, Brighton, 414 (1969).
90. A. J. McEvily, R. Kumble, and R. J. Donahue, to be published.
91. P. G. Forrest and A. E. L. Tate, J. of the Inst. of Metals, 93, 438 (1964-65).
92. A. J. McEvily, to be published.

LIST OF FIGURE TITLES

- Fig. 1. Effect of environment on fatigue properties of a 0.35% carbon steel. [2].
- Fig. 2. Co-ordinates and stress components in the crack tip stress field.
- Fig. 3. Compatibility data for 7075-T6 upon intensity factor. (High strength aluminum alloy).
- Fig. 4. The effect of water and water vapor on the rate of fatigue crack growth in 7075 aluminum alloy.
- Fig. 5. Effect of water vapor pressure on the rate of fatigue crack growth in a Al-Cu-Mg-alloy at 1 C/S.
- Fig. 6. Effect of specimen thickness on environmental sensitivity of the rate of fatigue crack growth. [61].
- Fig. 7. Comparison of the rate of fatigue crack growth of two aluminum alloys tested in air.
- Fig. 8. Effect of humidity on the rate of fatigue crack growth at two R levels.
- Fig. 9. Schematic fatigue crack growth rate plot.
- Fig. 10. Types of fatigue crack growth behavior.
- Fig. 11. Schematic illustration of the deformation at a fatigue crack tip during one loading cycle.
- Fig. 12. Comparison of experimental and predicted (Eq. 2, $A = 0.02$, $K_{TH} = 3 \text{ ksi}\sqrt{\text{in}}$) fatigue crack growth rates for 2024-T3 aluminum alloy.
- Fig. 13. Comparison of predicted values for the rate of fatigue crack growth with experimental results for a high strength steel.
- Fig. 14. Crack length, a , as a function of number of cycles, N , at three stress levels ($R = 0$ loading). Terminal point corresponds to a growth rate of 10^{-4} inches per cycle. a taken as 0.03 in. (Based on Eq. 7, with $A = 0.02$ and $K_{TH} = 3 \text{ ksi}\sqrt{\text{in}}$; 2024-T3 aluminum alloy).
- Fig. 15. Idealized "Goodman" diagram for fatigue crack growth rates.
- Fig. 16. Schematic crack growth curves.
- Fig. 17. Experimental and calculated fatigue curves for the aluminum alloy 2024-T3, $R = 0$. (Calculations based on Eqs. 12 and 13, with $A = 0.02$ and $K_{TH} = 3 \text{ ksi}\sqrt{\text{in}}$).

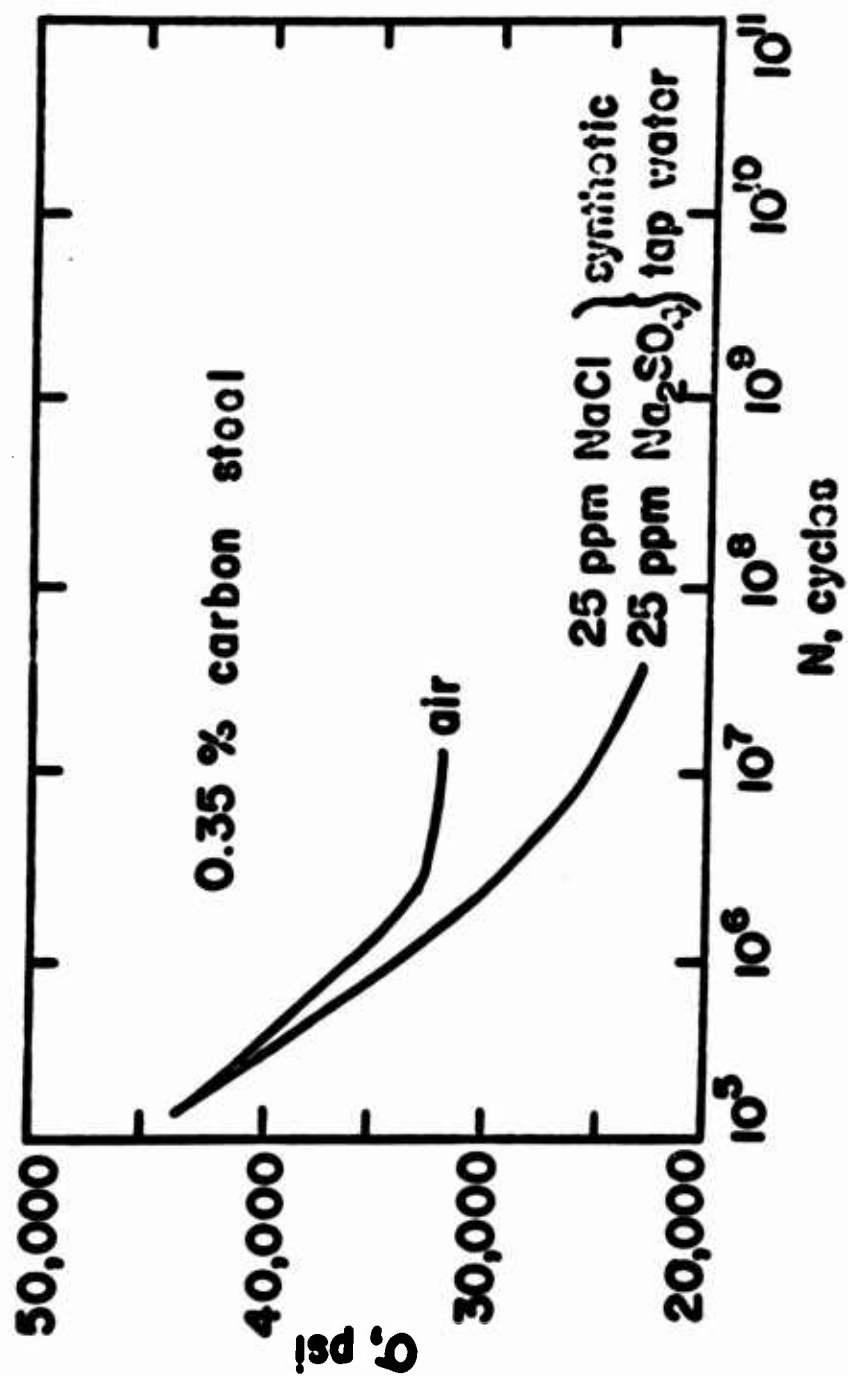


Fig. 1. Effect of environment on fatigue properties of a 0.35% carbon steel. [2].

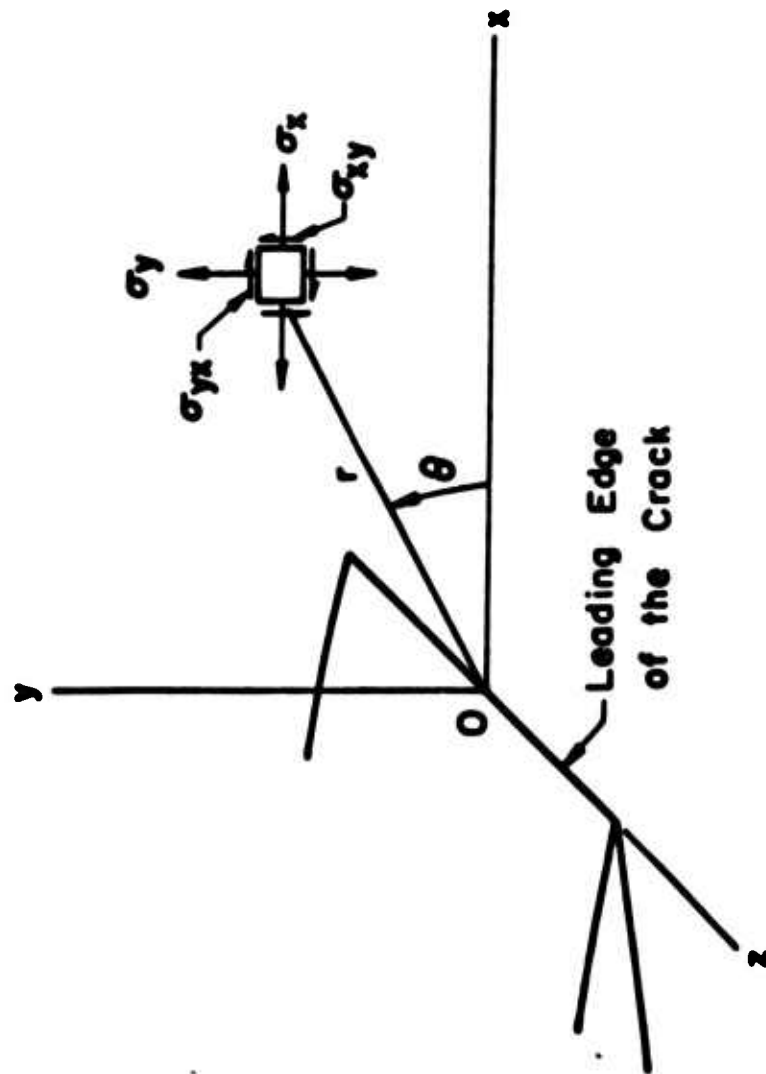


Fig. 2. Co-ordinates and stress components in the crack tip stress field.

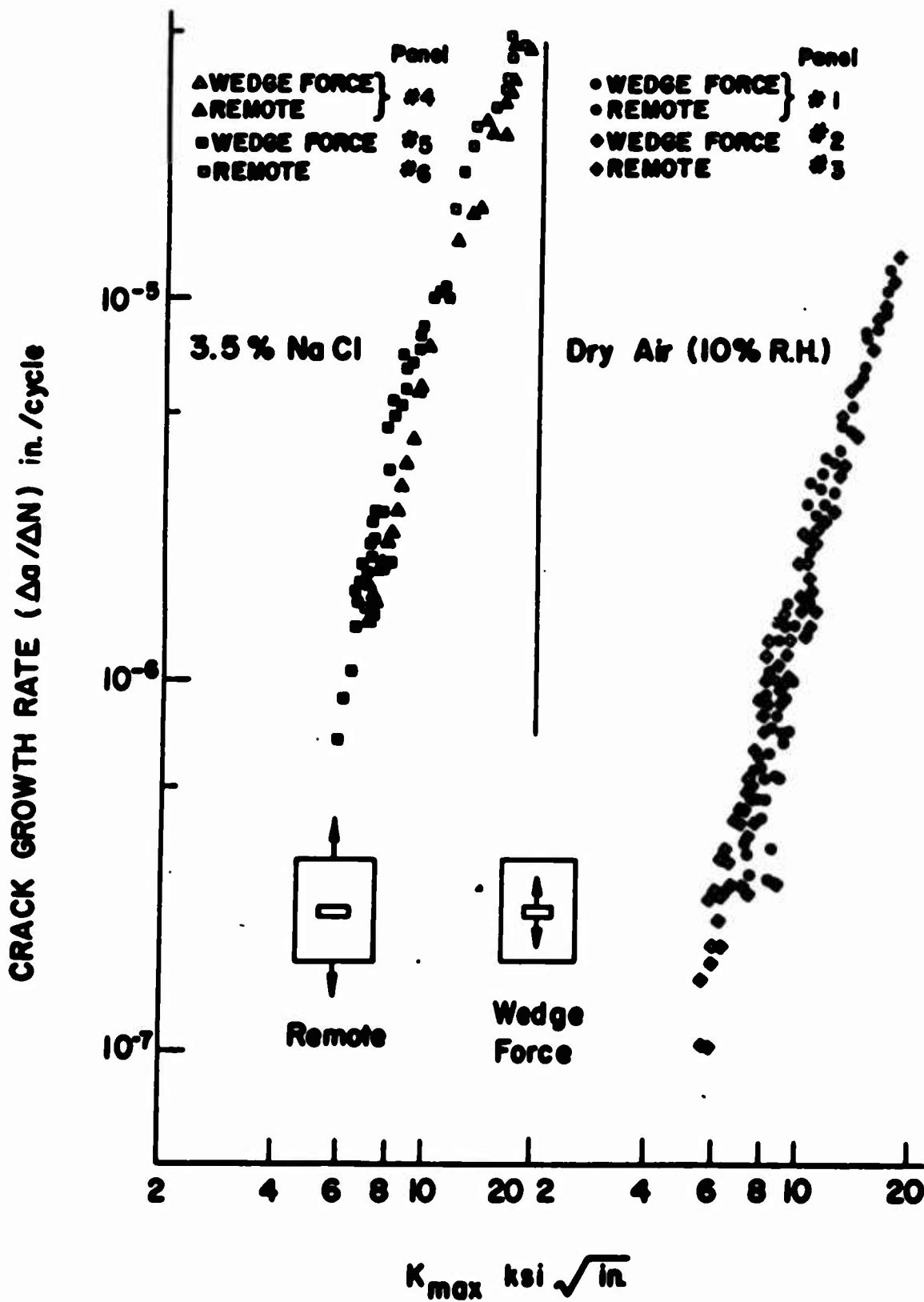


Fig. 3. Compatibility data for 7075-T6 upon intensity factor.
 (High strength aluminum alloy).

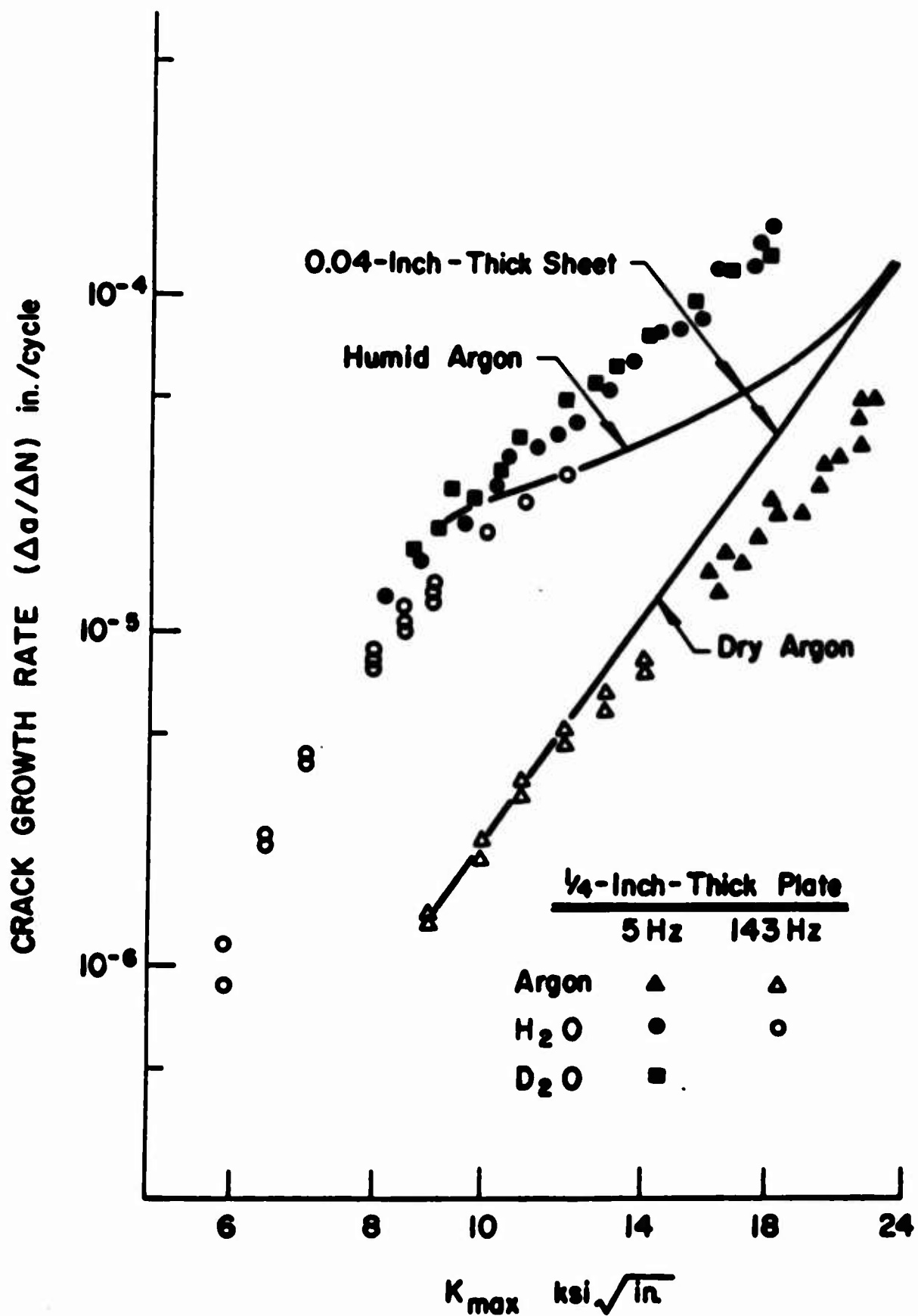


Fig. 4. The effect of water and water vapor on the rate of fatigue crack growth in 7075 aluminum alloy.

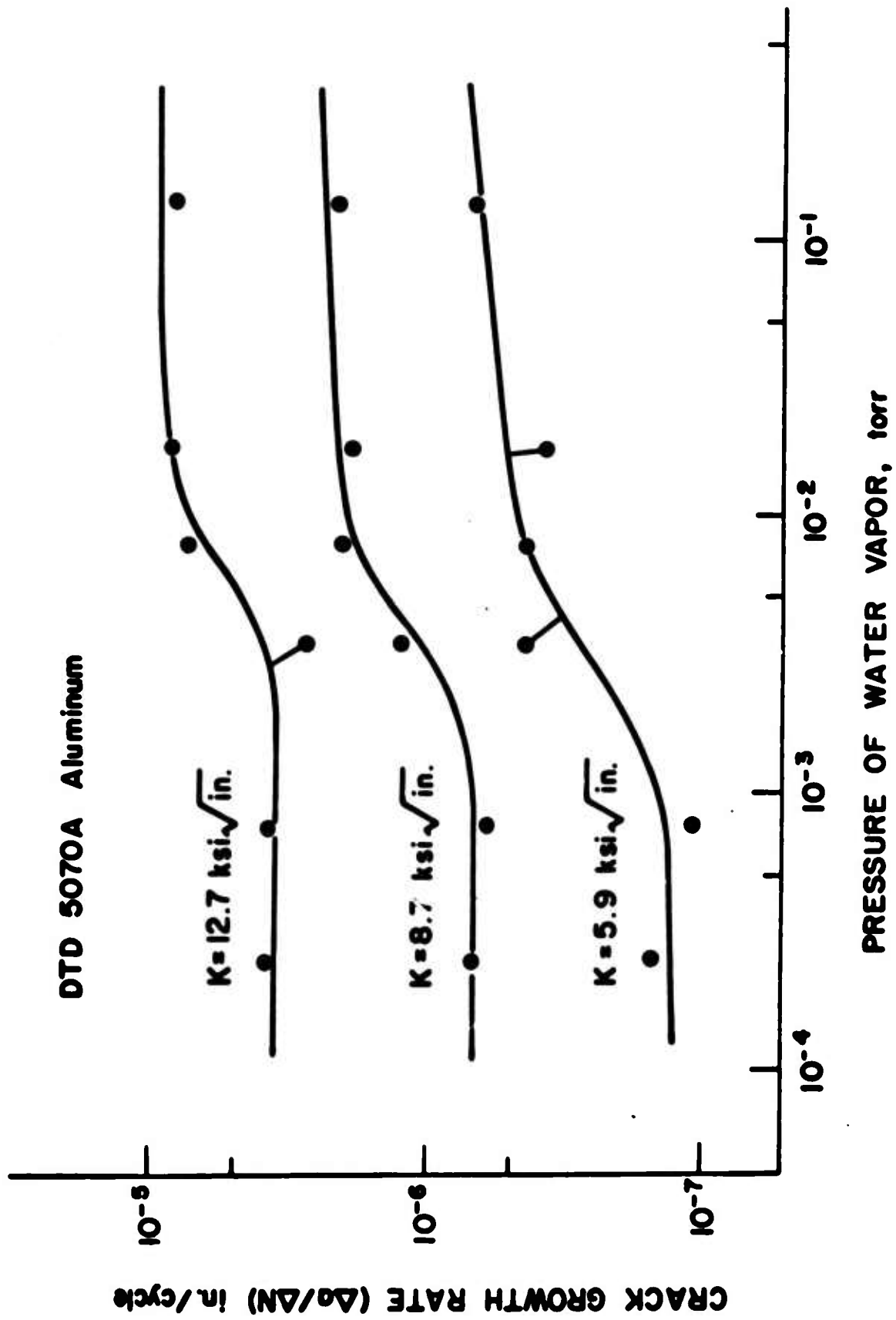


Fig. 5. Effect of water vapor pressure on the rate of fatigue crack growth in a Al-Cu-Mg-alloy at 1 C/S.

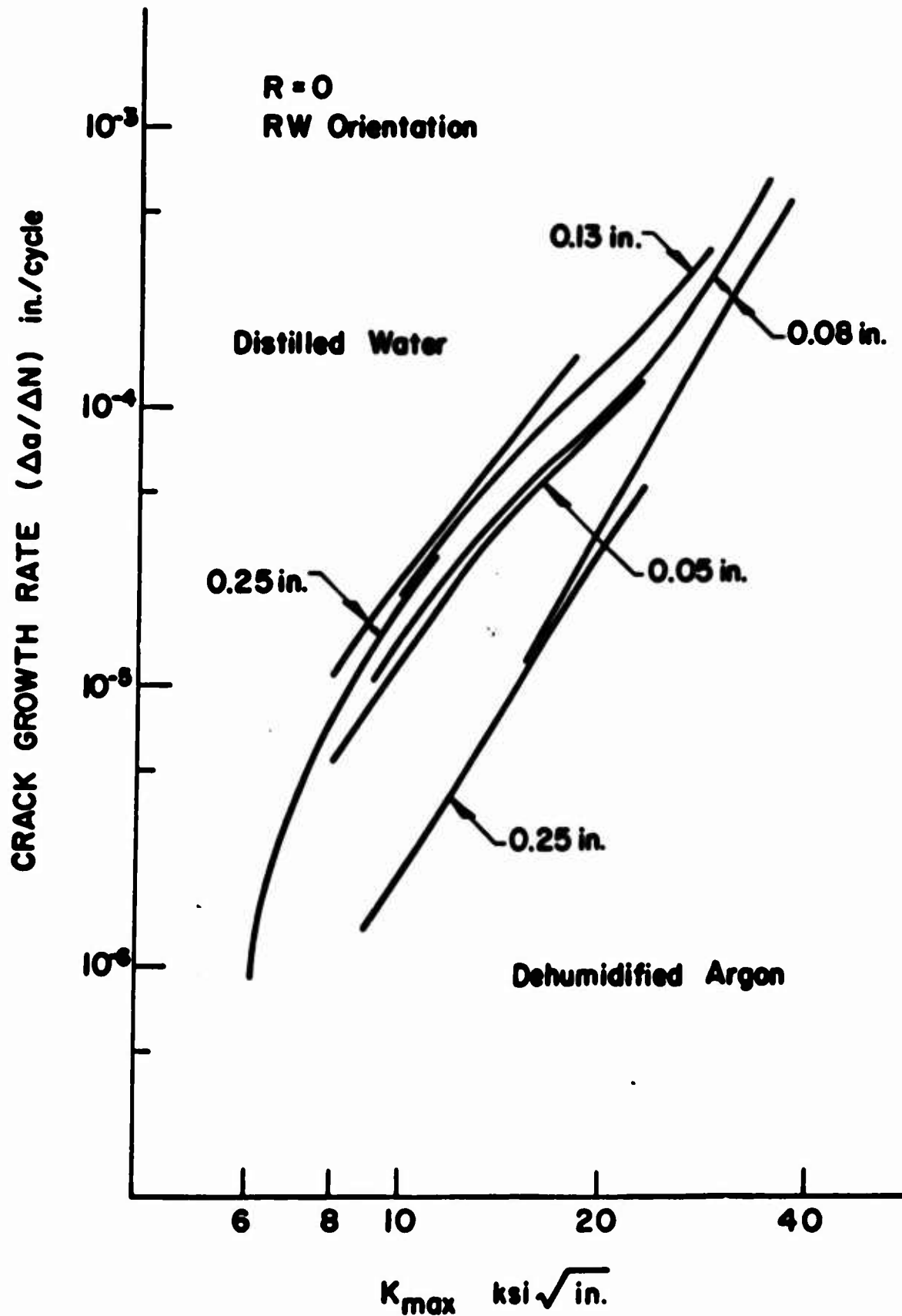


Fig. 6. Effect of specimen thickness on environmental sensitivity of the rate of fatigue crack growth. [61].

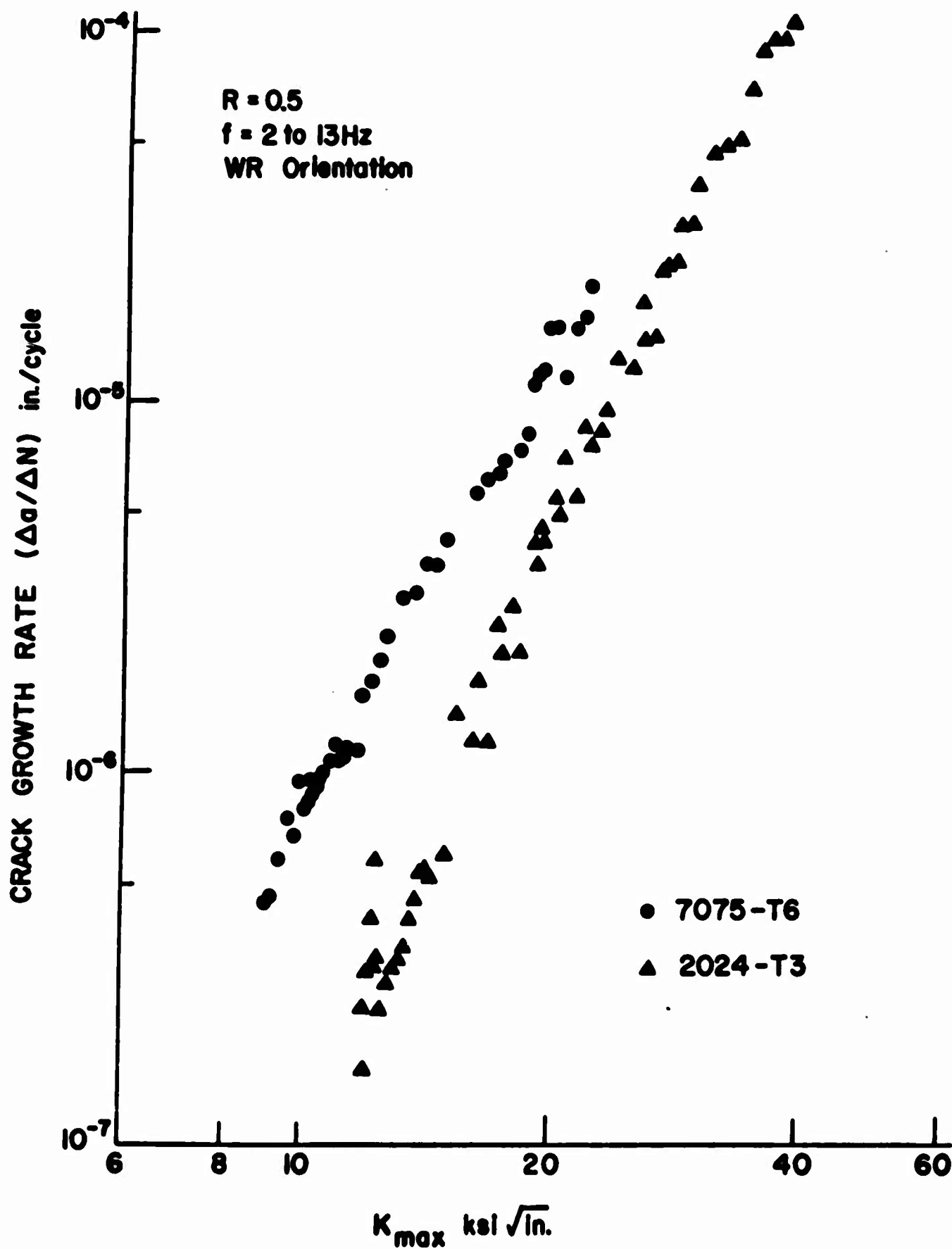


Fig. 7. Comparison of the rate of fatigue crack growth of two aluminum alloys tested in air.

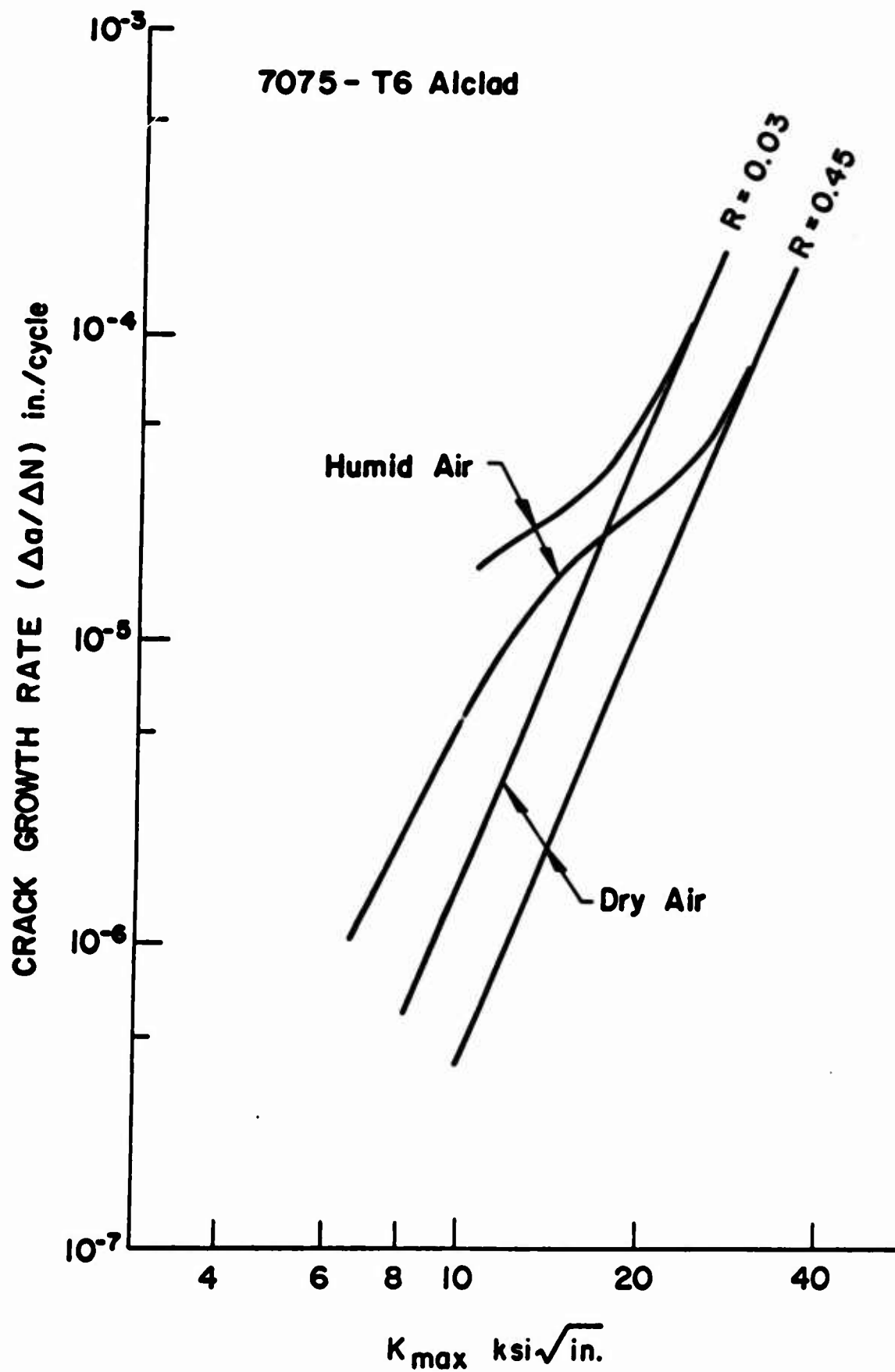


Fig. 8. Effect of humidity on the rate of fatigue crack growth at two R levels.

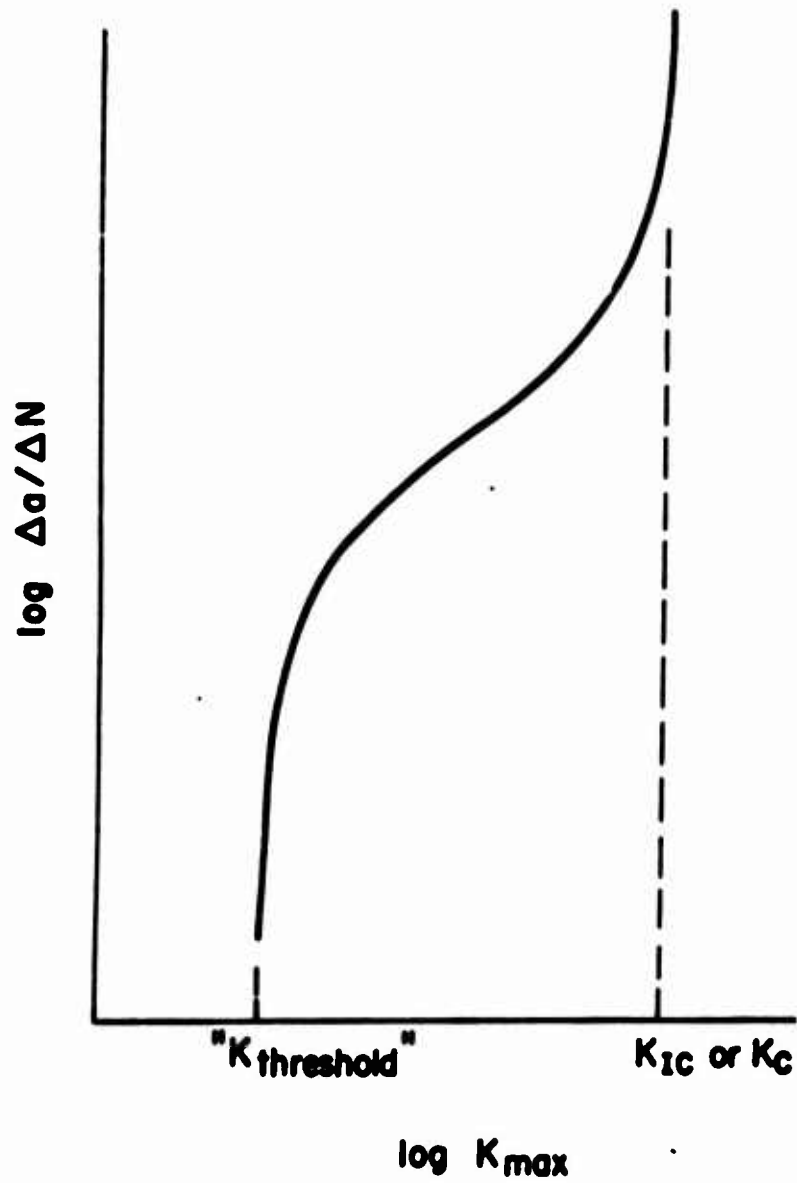


Fig. 9. Schematic fatigue crack growth rate plot.

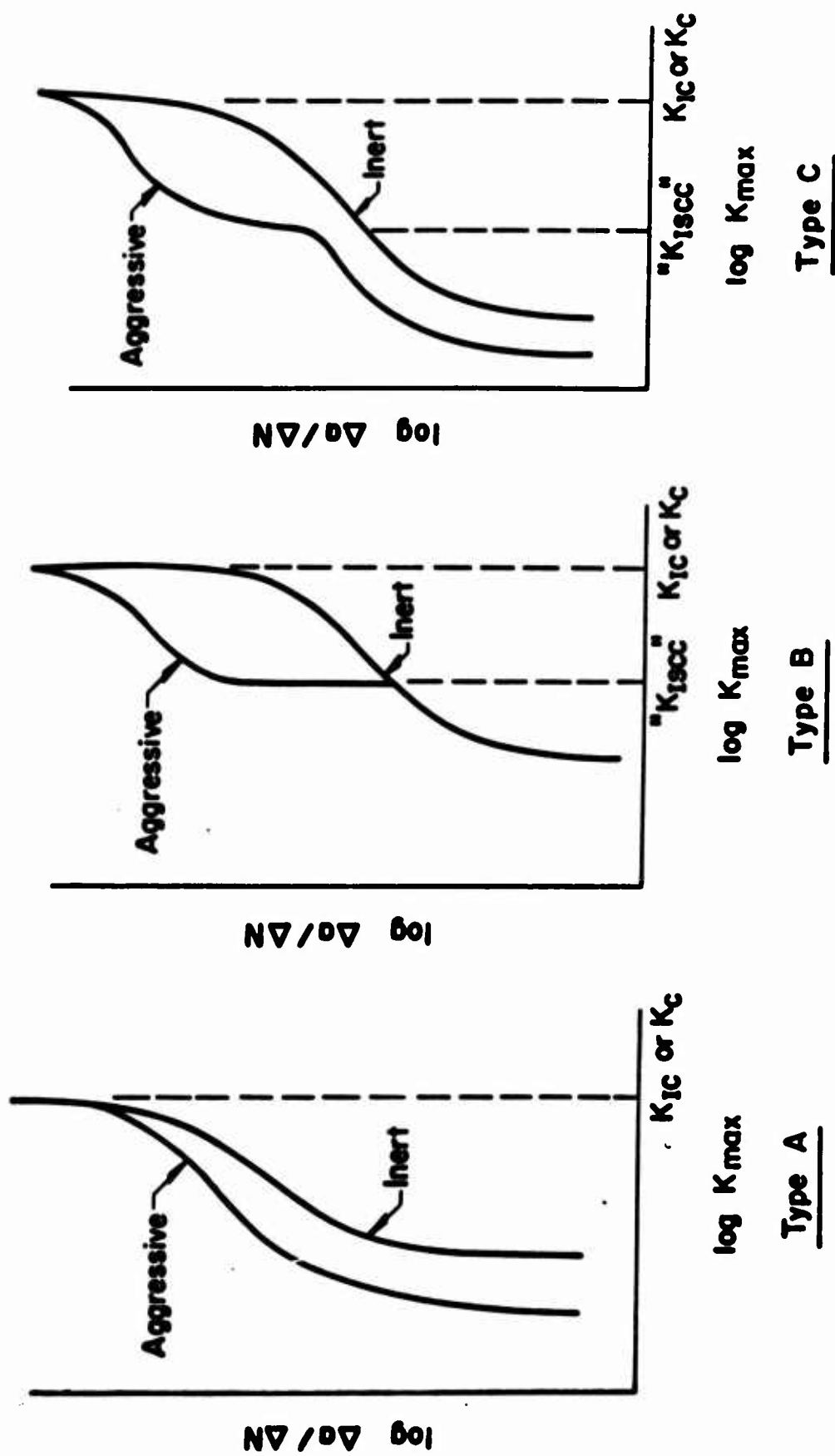


Fig. 10. Types of fatigue crack growth behavior.

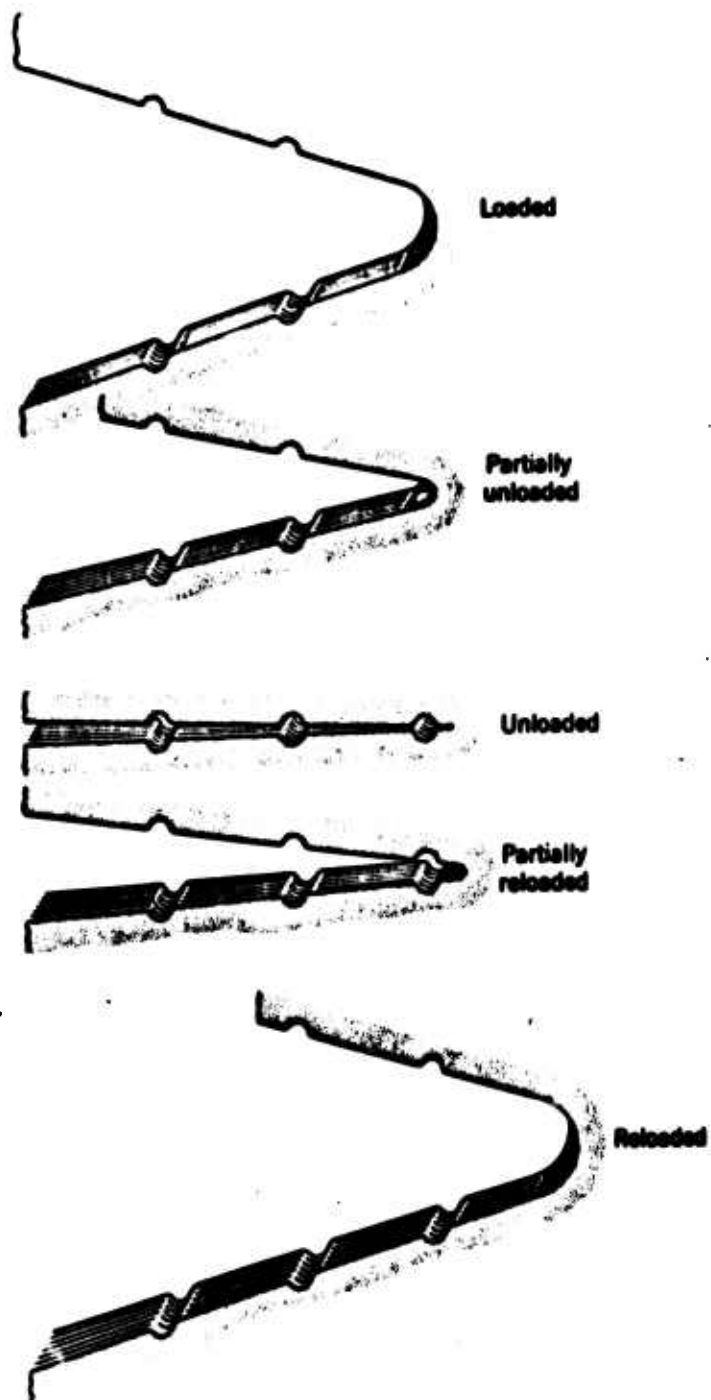


Fig. 11. Schematic illustration of the deformation at a fatigue crack tip during one loading cycle.

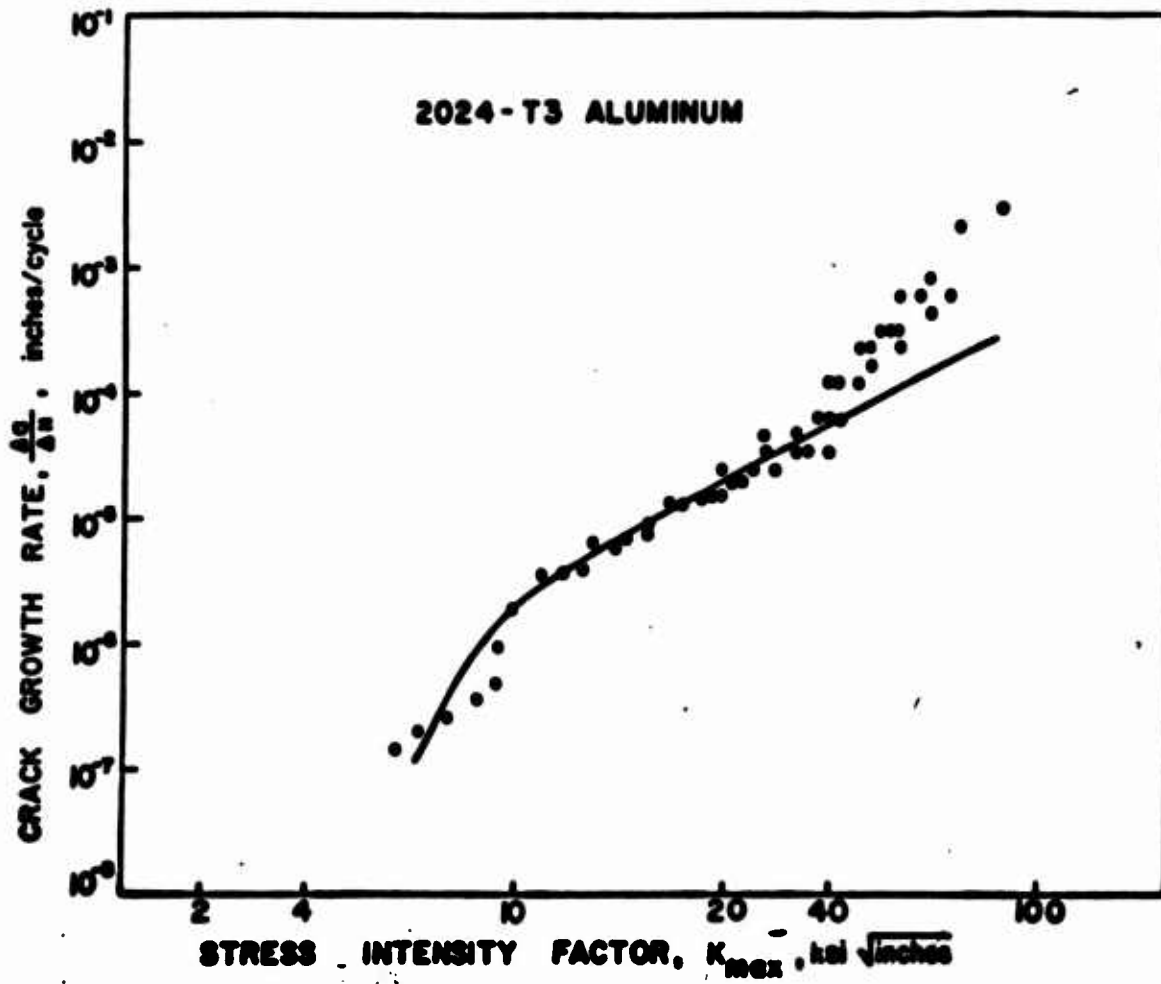


Fig. 12. Comparison of experimental and predicted (Eq. 2, $A = 0.02$, $K_{TH} = 3 \text{ ksi}\sqrt{\text{in}}$) fatigue crack growth rates for 2024-T3TH aluminum alloy.

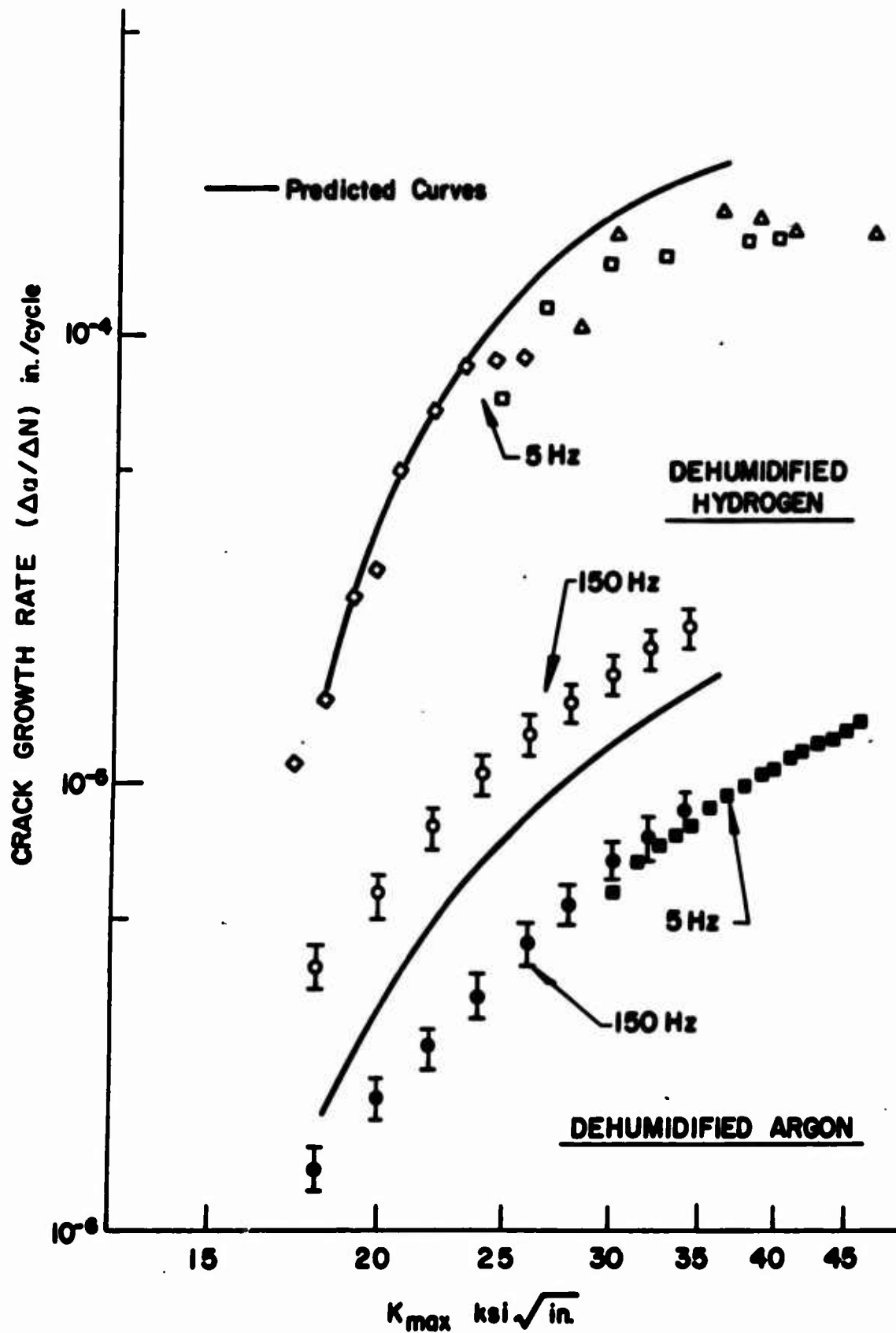


Fig. 13. Comparison of predicted values for the rate of fatigue crack growth with experimental results for a high strength steel.

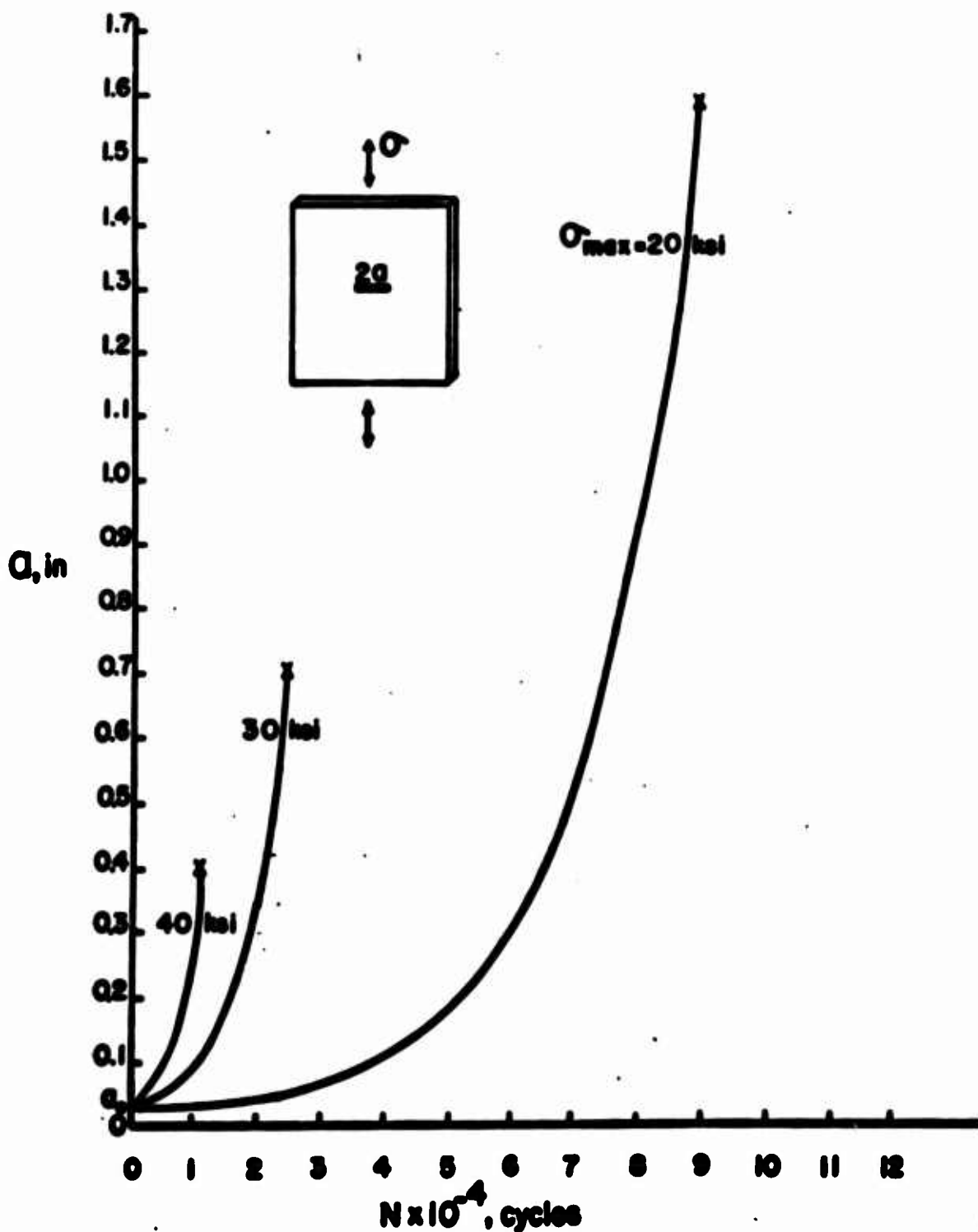


Fig. 14. Crack length, a , as a function of number of cycles, N , at three stress levels ($R = 0$ loading). Terminal point corresponds to a growth rate of 10^{-4} inches per cycle. a taken as 0.03 in. (Based on Eq. 7, with $A = 0.02$ and $K_{TH} = 3 \text{ ksi}/\sqrt{\text{in}}$; 2024-T3 aluminum alloy).

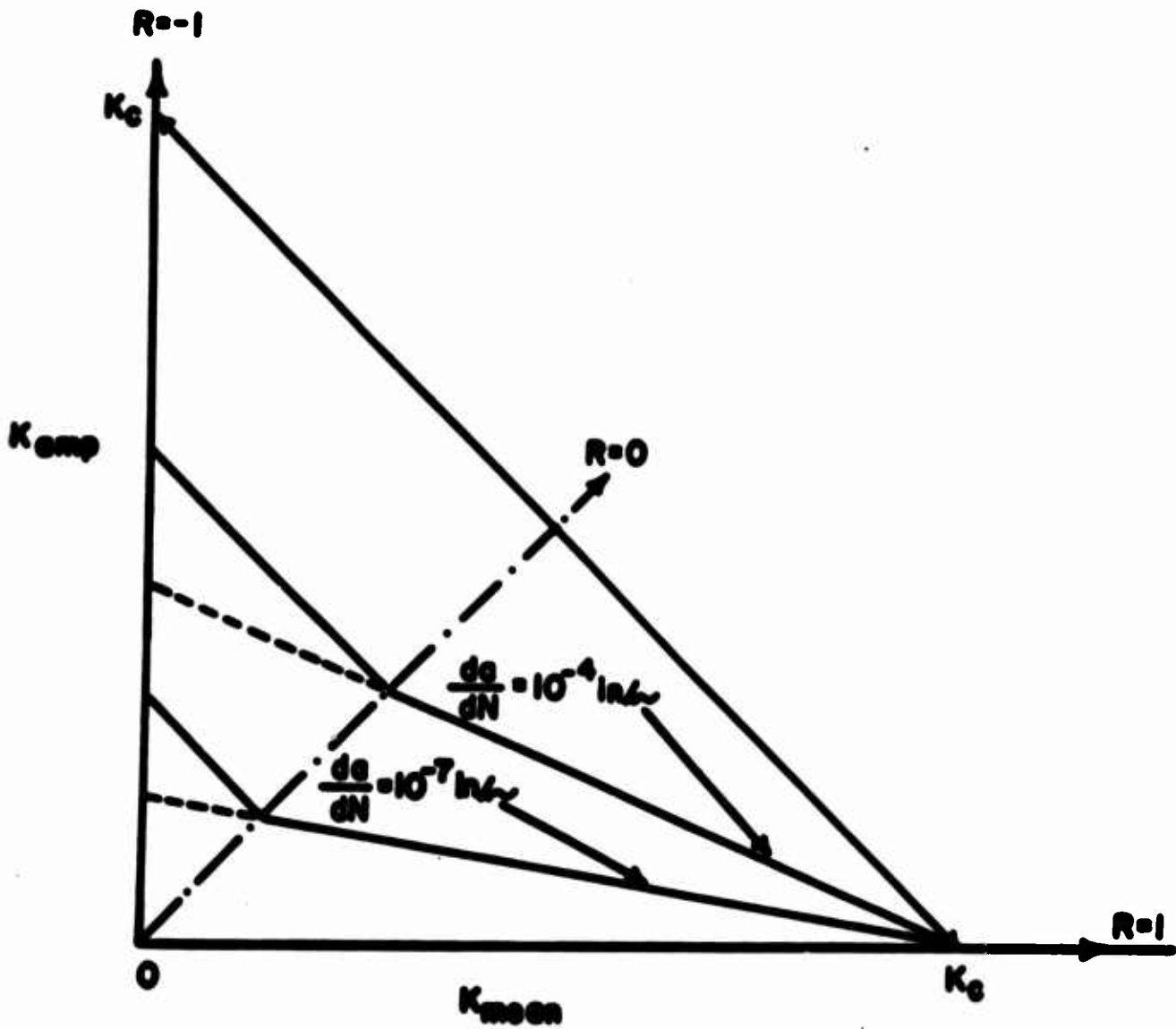


Fig. 15. Idealized "Goodman" diagram for fatigue crack growth rates.

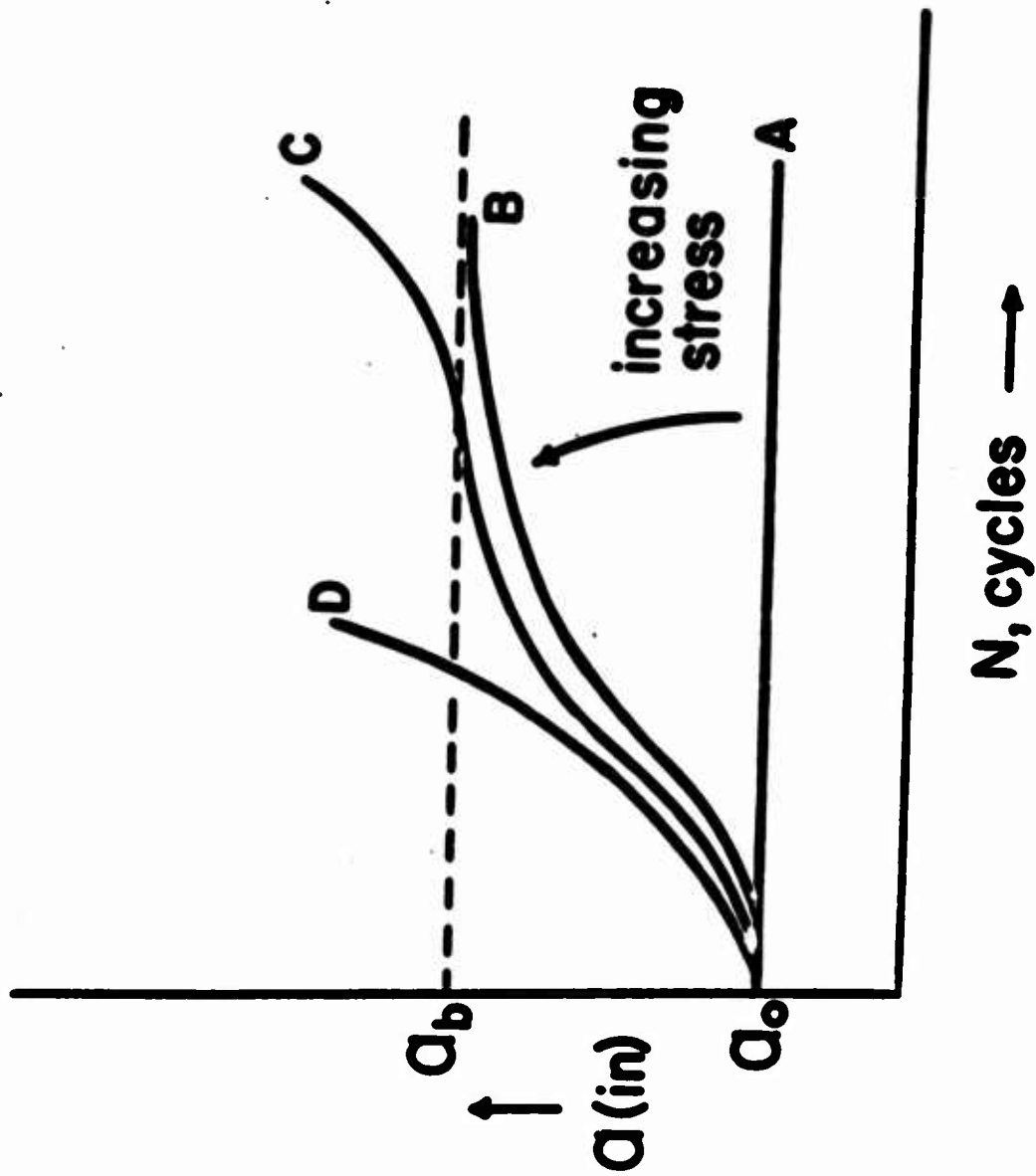


Fig. 16. Schematic crack growth curves.

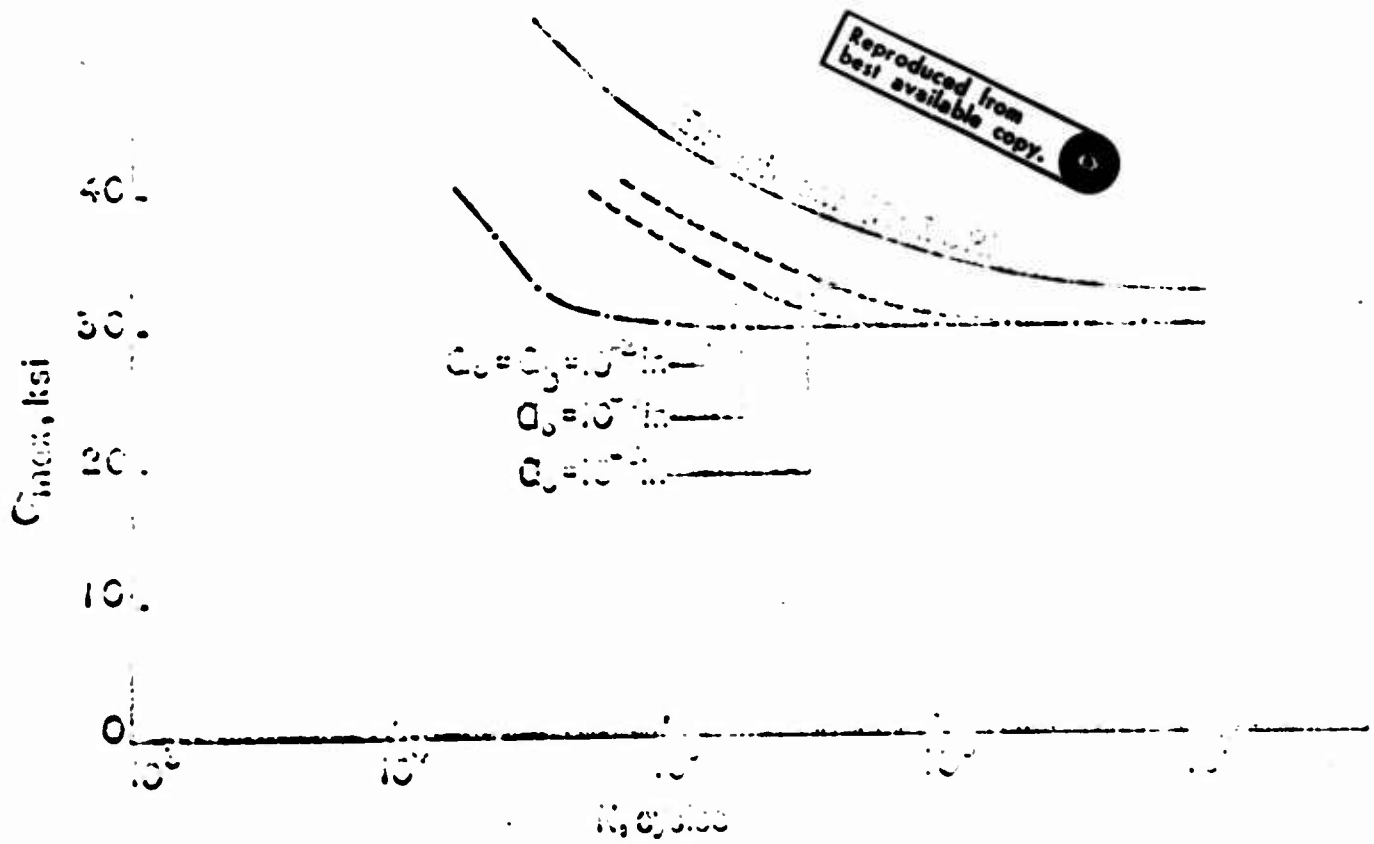


Fig. 17. Experimental and calculated fatigue curves for the aluminum alloy 2024-T3, $R = 0$. (Calculations based on Eqs. 12 and 13, with $\lambda = 0.02$ and $K_{T\lambda} = 3$ ksi/in.).

INSTITUTE OF MATERIALS SCIENCE

The Institute of Materials Science was established at The University of Connecticut in 1966 in order to promote the various fields of materials science. To this end, the State of Connecticut appropriated \$5,000,000 to set up new laboratory facilities, including approximately \$2,150,000 for scientific equipment. In addition, an annual budget of several hundred thousand dollars is provided by the State Legislature to support faculty and graduate student salaries, supplies and commodities, and supporting facilities such as various shops, technicians, secretaries, etc.

IMS fosters interdisciplinary graduate programs on the Storrs campus and at present is supporting five such programs in Alloy Physics, Biomaterials, Crystal Science, Metallurgy, and Polymer Science. These programs are directed toward training graduate students while advancing the frontiers of our knowledge in technically important areas.